ELSEVIER

Coordination Chemistry Reviews
210 (2000) 135–179

COORDINATION CHEMISTRY REVIEWS

www.elsevier.com/locate/ccr

Thiolates, selenolates, and tellurolates of the s-block elements

Ulrich Englich, Karin Ruhlandt-Senge *

Department of Chemistry and W.M. Keck Center for Molecular Electronics, 1-014 Center for Science and Technology, Syracuse University, Syracuse, NY 13244-4100, USA

Received 8 October 1999; accepted 15 December 1999

Contents

* Corresponding author. Tel.: +1-315-4432925; fax: +1-315-4434070.
E-mail address: kruhland@syr.edu (K. Ruhlandt-Senge).

PII: S0010-8545(00)00319-2

Abstract

The potential of alkali and alkaline earth metal chalcogenolates in synthetic chemistry and various technical applications has sparked the recent interest in the chemistry of alkali and alkaline earth metal thiolates, selenolates and tellurolates. As a result, an increasing body of work concerned with exploring synthetic routes to the target compounds, analyzing the influence of metal, ligand and donor on the structural chemistry, and correlating structure and function has appeared in the literature, most of which during the last few years. This article describes recent trends in this area of alkali and alkaline earth chemistry, by discussing synthetic access routes, analyzing structure determining factors such as metal, donor and ligand influence, comparing structural similarities and disparities in alkali and alkaline earth chemistry, and discussing structure–function relationships.

Keywords: Alkali metals; Alkaline earth metals; Thiolates; Selenolates; Tellurolates; Structural chemistry; Structure–function relationship

1. Introduction

Alkali and alkaline earth metal chalcogenolates have important uses in synthetic and technical chemistry. Their widespread applications resulted in considerable interest in their structural chemistry, and over the last decade a steadily increasing number of target molecules have been reported.

Review articles on the subject have been disseminated by Setzer and von Ragué Schleyer on lithium compounds with a coverage until 1983 and partial listing for 1984 [1], Dilworth and Hu [2], describing the chemistry of sterically hindered thiolates until 1991 and part of 1992, Pauer and Power discussing lithium chemistry until 1992 and parts of 1993 [3], Arnold, summarizing tellurolate chemistry until 1994 [4], Janssen, Grove and van Koten, reporting on lithium and magnesium thiolates until 1995 [5], and Ruhlandt-Senge covering the alkaline earth chalcogenolate literature until 1996 [6].

Chemistry based on the alkali and alkaline earth metal–oxygen bonds has been the most thoroughly developed and continues to be an active area of research [3,7–16]. In marked contrast, considerably less attention has been paid to develop synthetic strategies towards the corresponding thiolates, selenolates, and tellurolates and to elucidate their solution and solid-state structures. This has been expressively demonstrated by Pauer and Power comparing the number of lithium alkoxides, aryloxides, enolates, and heterometallic species (69 total), with only 21 thiolates, selenolates and tellurolates combined [3].

The structural chemistry of alkali and alkaline earth metal chalcogenolates dates back to 1972, with the first powder diffraction study on ASMe (A = Li, Na, K) [17]. Single crystal data on lithium thiolates were first published in 1985 [18], structural data on the first lithium selenolate in 1991 [19,20], and those of the first tellurolate in 1992 [21,22]. Single crystal data on sodium and potassium thiolates appeared in the literature in 1991 [23], the first rubidium and cesium thiolates were published as

late as 1996 [24]. Analogous to alkali metal chalcogenolates, corresponding alkaline earth chemistry has experienced a rapid growth during the last decade, beginning with the structural characterization of the first magnesium thiolate in 1990 [25], magnesium and calcium tellurolates in 1992 [26,27], a beryllium thiolate in 1993 [28], strontium selenolate in 1994, and the first barium tellurolate in 1994 [29]. Since then, a rapidly growing number of target compounds has appeared in the literature, most of them during the last 2 to 3 years.

The recent interest in the chemistry of alkali and alkaline earth metal chalcogenolates was sparked by their central role in organic and inorganic synthetic chemistry, but also by the discovery of strontium and barium containing high-temperature superconductors. Since then a large volume of strontium and barium oxygen derivatives have been reported [7–16]. The heavier chalcogen derivatives have received less attention, despite their importance in the production of wide band gap semiconductors [30–33], two- color IR optical windows [34–36], and phosphor materials [37]. Specifically, the band gap of conventional IIB-VIA materials can be modulated by alkaline earth metal inclusion, as demonstrated with the incorporation of magnesium into ZnS/ZnSe phases. The novel, quaternary ZnMgSSe material made possible the first continuous wave operation of blue–green laser diodes at room temperature. The importance of alkaline earth chalcogenolates also extends towards applications in synthetic chemistry. Specifically, magnesium thiolates, selenolates and tellurolates are useful in metathesis reactions as shown with the synthesis of $Cp_2M(TeSi(SiMe_3)_3)_2$ (M = Ti, Zr) [27]. Moreover, the heterobimetallic thiolate $[Cu_4Mes_4][Mg(SR)_2]_2$ (R = 2-((*R*)CH(Me)$NMe_2C_6H_4$)), comprised of two magnesium thiolate units bound to a central tetranuclear cuprate moiety, has been related to Cu(I) catalyzed conjugate 1,4-addition of Grignard reagents to enones and other regio- and stereospecific C–C bond forming processes [5,25].

Since structural factors critically affect physical properties and consequently the suitability of the target compounds in various applications, detailed investigations into factors modulating structural parameters are warranted. Of specific interest are variables determining aggregation chemistry, but possibly even more critical is information on how association in both solution and the solid state can be directed. As a consequence, multiple studies have been undertaken to investigate the role of metal, ligand, solvent, and donors on the structural chemistry of alkali and alkaline earth metal chalcogenolates. This information is crucial in the design of improved synthetic reagents and precursor materials.

The interaction between the alkali and alkaline earth metals with the chalcogenolate ligands is closely related. Accordingly, variables affecting structure and function in these complexes are very comparable and triggered by identical factors. This article will shed light into similarities and disparities between the two groups of compounds.

The bonding in alkali and alkaline earth chalcogenolates may be described as covalent with a high ionic component. This view is supported by ab initio calculations performed by Pappas [38], who describes the interaction between alkali or alkaline earth cation and chalcogenolate anion(s) as mainly electrostatic. The highly polarized bond between the metal and chalcogenolate ligand(s) results in

distinct structural features in the target compounds. The degree of ionicity will decrease if elements of lower electronegativity are connected to the metal center. As such, tellurolates will exhibit the highest degree of covalency. The influence of subtle changes in covalency on structural parameters will be analyzed.

In addition to covalency considerations, many other parameters contribute towards the structural chemistry of the target compounds: ligand size, the nature of the chalcogen atom, base strength, size and hapticity of the donor, as well as the charge density of the metal center. In most instances, the structural features observed in the target compounds are consequences of several contributing factors. Monomeric species are generally available, if sterically demanding ligands and/or strongly coordinating or multidentate bases are used. If however the interaction of the base with the metal center is stronger than that of the ligand, separation of anion and cation may be induced. Alkali metal complexes may display two-ion association modes: one with metal–ligand interaction, one with separated ions. Alkaline earth derivatives may exhibit three different cation–anion association types: with two, one or no contact(s) between metal and ligand (Scheme 1).

Higher aggregates are observed if the ligand size is reduced, weaker bases are employed, or the donor is utilized in limited quantity, or not at all. Accordingly, the metal center interacts with a neighboring ligand to saturate its coordination sphere, and dimeric, trimeric, or higher oligomers containing bridging chalcogenolate functionalities will be observed. The ability to adopt bridging moieties chiefly depends on bond strength considerations. Since bond strength decreases upon descending a group, higher aggregates are most likely to be observed for the lighter congeners. In contrast, the increased radial extension of the heavier metal centers requires increased steric presence to saturate the metals' coordination environment. Accordingly, higher aggregates may also be observed for the heavier derivatives, especially, if small ligands are utilized.

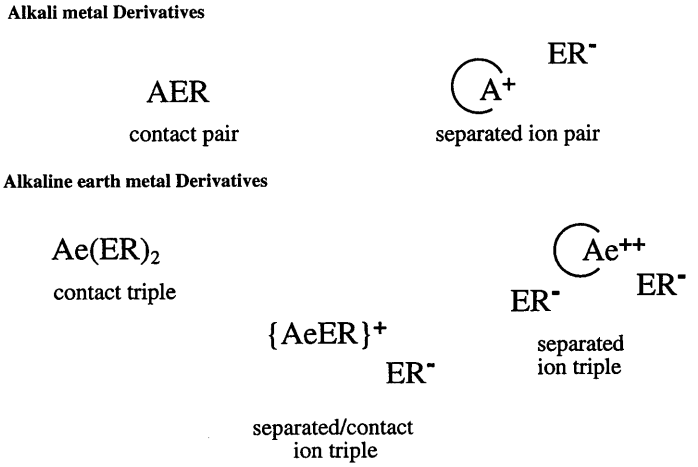

Scheme 1. Ion association modes in alkali and alkaline earth metal chalcogenolates.

This article will discuss important structural trends observed in alkali and alkaline earth chalcogenolate chemistry. A specific focus of the discussions will include: (1) similarities and disparities among alkali and alkaline earth elements; (2) the influence of metal, ligand and donor on the structural outcome; and (3) structure–function relationships in the target compounds.

The major source of information for this article is the Cambridge Structural Database with its most recent release from April 1999 [39]. Recent data from the primary literature (including summer 1999) and unpublished data from our laboratory are also provided. This review article is limited to simple thiolates, selenolates and tellurolates, including intramolecular stabilized chalcogenolates, such as pyridine thiolates or one and two armed pincer ligands. The vast group of compounds bearing thiocarboxylates and related ligands have been summarized in a recent comprehensive review article [40].

2. Alkali metal thiolates, selenolates and tellurolates

2.1. Synthetic aspects

Synthetic routes towards alkali metal thiolates, selenolates and tellurolates are summarized in Scheme 2.

Type of reaction:	Equation:	used for:
Hydrogen elimination	$AH + HER \longrightarrow AER + H_2$	Na, K
Alkane elimination	$nBuLi + HER \longrightarrow LiER + nBuH$	Li
Metallation	$A + HER \longrightarrow AER + {}^1/_2 H_2$	Na, K, Rb, Cs

E = S, Se, Te, R= alkyl, aryl, silyl, A = Na, K, Rb, Cs

Scheme 2. Synthetic routes to alkali metal chalcogenolates.

Lithium derivatives can be most conveniently prepared by reacting the chalcogenols with ^{n}BuLi. The reaction generally proceeds smoothly under extrusion of butane. A significant advantage is the suitability of a wide variety of ligands and donors [41]. Sodium and potassium derivatives are most conveniently available by the reaction of the corresponding hydrides with the chalcogenol acids. The hydride route generally proceeds smoothly, if a suitable Lewis donor is present in the reaction mixture [42]. Synthetic schemes involving organometallic sodium and potassium derivatives are not feasible, due to experimental difficulties connected with the preparation of the organometallic derivatives [43]. Rubidium and cesium species may be prepared by the reaction of the acids with the metals [24]. The high reactivity of the heavy alkali metals ensures a smooth reaction, while requiring experimental care. The low solubility of rubidium and cesium hydrides precludes their use in synthetic applications.

2.2. Lithium compounds

The structural chemistry of lithium thiolates, selenolates and tellurolates has been summarized in 1995 covering the literature until 1992 and parts of 1993 [3]. The number of lithium thiolates listed in this review was nine, in addition to four mixed metal thiolates. Van Koten et al. report in a review article covering the literature until 1995, 14 lithium thiolates, in addition to four mixed metal compounds [5]. This increase of well-characterized lithium thiolates demonstrates the continued interest in these compounds. During the last few years this trend has continued, adding a selection of new compounds to the steadily growing list. Table 1 summarizes selected structural data on lithium thiolates, selenolates and tellurolates.

The most common structural features observed for lithium thiolates, selenolates and tellurolates are monomeric and dimeric formulations, as shown in Figs. 1 and 2 (see Table 2 for geometrical details).

Novel developments in lithium chalcogenolate chemistry focus chiefly on compounds displaying higher degrees of aggregation, as observed in the trimeric thiolates $[Li(THF)SMes^*]_3$ [41], and $[LiS\text{-}2,6\text{-}Mes_2C_6H_2]_3$ [24], shown in Figs. 3 and 4, the tetramer $[LiS\text{-}2,4,6\text{-}Ph_3C_6H_2]_4$ [24] (Fig. 5), and some hexameric species, including $[LiS\text{-}2,6\text{-}((R)CH(Me)NMe_2)_2C_6H_3]_6$ [45] (Fig. 6), displaying a 12-membered ring comprised of alternating lithium and sulfur centers.

Other hexameric species include $[LiS\text{-}2\text{-}((R)CH(Me)NMe_2)C_6H_4]_6$ [45], exhibiting a hexagonal prismatic geometry analogous to the tellurolate $[LiTeSi(SiMe_3)_3]_6$ (Fig. 7) [73]. The isolation of the hexagonal prismatic thiolate was made possible by utilizing a 'one-armed pincer' ligand, providing a single intermolecular stabilization of the metal center. If a 'two-armed pincer' ligand, with two intramolecular

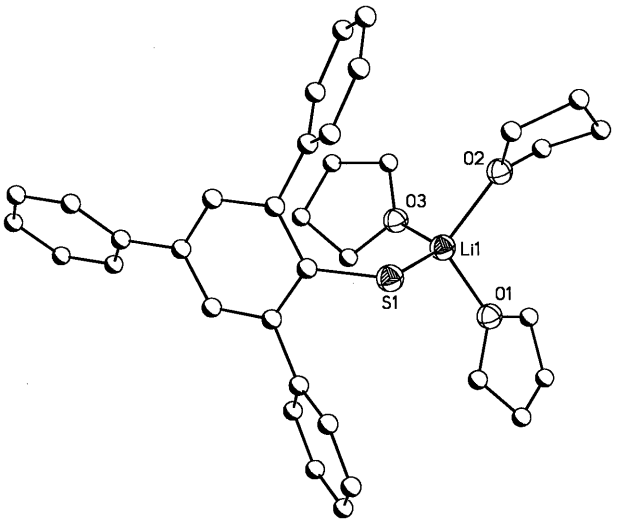

Fig. 1. Graphical representation of $Li(THF)_3Triph$. Hydrogen atoms have been omitted for clarity.

Table 1
Geometrical details of lithium thiolates, selenolates, and tellurolates

Compound	E	Aggr.	CN	Li–E (Å)	D	Li–D (Å)	Ref.
Li(PMDTA)STrip	S	1	4	2.37	PMDTA	2.14	[41]
$Li(py)_3S\text{-}2\text{-}Me\text{–}C_6H_4$	S	1	4	2.41	py	2.08	[44]
$[Li_2(THF)_2(S\text{-}2,6\text{-}CH_2NMe_2C_6H_3)I]$	S	1	4	2.41	N[a]	2.08	[45]
					THF	1.92	
$Li(THF)_3STriph$	S	1	4	2.43	THF	1.95	[46]
$Li(THF)_3SMes^*$	S	1	4	2.45	THF	1.97	[47]
$Li(HMPA)_2(H_2 2,4,6\text{-}S_3C_3N_3)$	S	1	4	2.96	N[a]	2.08	[48]
					HMPA	1.86	
$Li(PMDTA)SCPh_3$	S	1	4+1[b]	2.41	PMDTA	2.12	[41]
$Li(12C4)SCPh_3$	S	1	5	2.40	12C4	1.90–2.45	[41]
$[\{Li(S\text{-}2\text{-}NC_5H_4)\}_2(18C6)]$	S	1	5	2.60	N[a]	2.06	[42]
					18C6	2.06	
$Li(15C5)SCPh_3$	S	1	6	2.50	15C5	2.31	[49]
$Li(12C4)(S\text{-}2\text{-}NC_5H_4)$	S	1	6	2.89	N[a]	2.00	[42]
					12C4	2.14	
$[LiS\text{-}2,6\text{-}Trip_2C_6H_3]_2$	S	2	2+ar	2.40	Arene	2.50–2.71	[24]
$[LiS\text{-}2,6\text{-}Trip_2C_6H_3]_2 \cdot tol$	S	2	2+ar	2.43	Arene	2.41–2.90	[24]
$[Li(THF)_2SCPh_3]_2$	S	2	4+2[b]	2.48	THF	2.16	[41]
$Li_2(THF)_{3.5}\{SC(SiMe_3)_3\}_2$	S	2	3.5[c]	2.34	THF	1.92	[18]
$[Li(S\text{-}2CH_2N(Me)CH_2CH_2OMe)C_6H_4)]_2$	S	2	4	2.43	O[a]	1.97	[45]
					N[a]	2.07	
$[Li(TMEDA)STrip]_2$	S	2	4	2.45	TMEDA	2.15	[41]
$[Li(THF)_2SCH(SiMe_3)_2]_2$	S	2	4	2.45	THF	1.95	[18]
$[Li(TMEDA)(SC(O)Ph)]_2$	S	2	4	2.48	O[a]	1.88	[50]
					TMEDA	2.16	
$[Li(TMEDA)(NC(S)SC_2H_4)]_2$	S	2	4	2.49	N[a]	2.04	[51]
					TMEDA	2.18	
$[Li(Et_2O)(S\text{-}2,6\text{-}Mes_2C_6H_3)]_2$	S	2	4	2.50	Et_2O	1.96	[52]
			2+ar	2.37	Arene	2.64–2.80	
$[Li(DME)]_2[Li\{(SiMe_3)_2C_5H_4S\text{-}2\}_2PPh]_2$	S	2	4	2.52	DME	1.98	[53]
$[Li(TMEDA)CH_2SPh]_2$	S	2	4	2.56	TMEDA	2.14	[54]
$[Li_2(HMPA)_3(NC(S)NC_6H_4)]_2$	S	2	4	2.68	N[a]	2.01	[51]
					HMPA	1.92	

Table 1 (*Continued*)

Compound	E	Aggr.	CN	Li–E (Å)	D	Li–D (Å)	Ref.
$[PhNLiC(=NPh)SLi \cdot 2HMPA]_2$	S	2	3,4	2.43	HMPA	1.84–1.97	[55]
$[LiS\text{-}2,6\text{-}(Mes)_2C_6H_3]_3$	S	3	2+ar	2.39	Arene	2.38–2.77	[24]
			3+ar	2.53	Arene	2.38–2.77	
$[Li(THF)(SMes^*)]_3$	S	3	3	2.36	THF	1.90	[41]
$[LiSTriph]_4$	S	4	2+ar	2.41	Arene	2.41–2.73	[24]
			3+ar	2.48	Arene	2.41–2.73	
$[Li(S\text{-}2,6\text{-}CH_2NMe_2C_6H_3)]_6$	S	6	4	2.41	N	2.15	[45]
$[Li(S\text{-}2\text{-}(R)\text{-}CH(Me)NMe_2C_6H_4)]_6$	S	6	4	2.42[d]	N	2.08	[45]
				2.55[e]			
$[Li(py)SCH_2Ph]_n$	S	*n*	4	2.48	py	2.06	[44]
$[Li(py)_2SPh]_n$	S	*n*	4	2.49	py	2.07	[44]
$[Li(HMPA)(NC(S)NC_3H_3)]_n$	S	*n*	4	2.80	N[a]	2.07	[51]
					HMPA	1.87	
$[Li(12C4)_2][SMes^*]$	S	–	8	–	12C4	2.18–2.49	[41]
$[Li(THF)_2]Zr(S'Bu)_6$	S	1	4	2.37	THF	1.88	[56]
				2.56			
$[\{Li(DME)\}_4U(SCH_2CH_2S)_4]$	S	1	4	2.24	DME	2.06	[57]
$[Li_3(TMEDA)_3Sm(S'Bu)_6]$	S	1	4	2.37	TMEDA	2.19	[58]
$[Li_3(TMEDA)_3Yb(S'Bu)_6]$	S	1	4	2.38	TMEDA	2.16	[58]
$Li(Et_2O)_2In(STrip)_4$	S	1	4	2.39	Et_2O	1.92	[59]
$Li(Et_2O)_2Ga(STrip)_4$	S	1	4	2.42	Et_2O	2.01	[59]
$Li(THF)_2\{S'Bu\}_2LuCp^*_2$	S	1	4	2.45	THF	1.95	[60,61]
$Li(THF)\{(ZrCp^*(SCH_2Ph)_2\}_2(SCH_2Ph)O$	S	1	4	2.47	THF	1.86	[62]
$[Li(Et_2O)]_2Ni(S'Bu)_4$	S	1	4	2.49	Et_2O	1.94	[63]
$Li(THF)_2Fe(SMes^*)_3$	S	1	4	2.57	THF	1.95	[64]
$[Li(THF)][V(S_3C_4H_8)_2]$	S	*n*	4	2.48	THF	2.00	[65]
			6	2.65			
$Li(THF)_3SeMes^*$	Se	1	4	2.57	THF	1.97	[19,20]
$Li(py)_2Yb(py)_2(SePh)_4$	Se	1	4	2.63	py	1.98	[66]

Table 1 (*Continued*)

Compound	E	Aggr.	CN	Li–E (Å)	D	Li–D (Å)	Ref.
$Li(THF)_2(SePh)_2LuCp_2$	Se	1	4	2.65	THF	1.90	[61]
$[Li(bipy)(SePh)]_2$	Se	2	4	2.57	bipy	2.04	[67]
$[Li(DME)SeSi(SiMe_3)_3]_2$	Se	2	4	2.59	DME	2.02	[68]
$[Li(bipy)(Se\text{-}2\text{-}NC_5H_4)]_2$	Se	2	4	2.62	bipy	2.09	[67]
$[Li(THF)SeMes^*]_3$	Se	3	3	2.47	THF	1.90	[69]
$Li(DME)Te\text{-}2\text{-}CH_2NMe_2C_6H_4$	Te	1	4	2.72	DME	1.95	[70]
$[Li(Te(\eta^5\text{-}C_5H_3(CH_2NMe_2)\text{-}2)Fe(\eta^5\text{-}C_5H_5))(DME)]$	Te	1	4	2.74	N[a]	2.08	[71]
					DME	1.98	
$Li(THF)_3TeMes^*$	Te	1	4	2.82	THF	1.95	[70]
$[Li(12C4)_2][TeSi(SiMe_3)_3]$	Te	1	8	–	12C4	2.33	[22]
$[Li(THF)TeSi(SiMe_3)_3]_2$	Te	2	3	2.74	THF	1.88	[72]
$[Li(DME)TeSi(SiMe_3)_3]_2$	Te	2	4	2.83	DME	2.00	[21]
$[Li(THF)_2TeSi(SiMe_3)_3]_2$	Te	2	4	2.85	THF	1.95	[22]
$[LiTeSi(SiMe_3)_3]_6$	Te	6	3	2.75	–	–	[73]

[a] Intramolecular coordination.
[b] Additional agostic interactions observed.
[c] Li is connected to THF with half occupancy.
[d] Within either top or bottom layer.
[e] Interaction between layers.

Table 2
Geometrical details of sodium thiolates, selenolates, and tellurolates

Compound	E	Aggr.	CN	Na–E (Å)	D	Na–D (Å)	Ref.
[Na(18C6)(S-2-NC_5H_4)]	S	1	6	2.76	N[a]	2.65	[42]
					18C6	2.45–3.02	
[Na(15C5)(S-2-NC_5H_4)]	S	1	7	3.04	N[a]	2.43	[42]
					15C5	2.51	
[Na(18C6)$(THF)_2$]SMes*	S	1	8	–	18C6	2.74	[75]
					THF	2.35	
[NaS-2,6-$Trip_2C_6H_3]_2 \cdot$ tol	S	2	2+ar	2.71	Arene	2.84–3.24	[24]
[Na(PMDTA)STrip]$_2$	S	2	5	2.83	PMDTA	2.54	[76]
[$(NaSSiPh_3)_6(tol)_2$]	S	6	3+ar	2.80	Arene	2.85–3.66	[49]
			4	2.94			
[Na(SC_5H_2N-3,6-($SiMe_2$-^{t}Bu)$_2$)]$_6$	S	6	4	2.82	N[a]	2.48	[77]
[Na($Et_2O)_{2/3}$STrip]$_6$	S	6	4	2.87	Et_2O	2.36	[76]
[Na(TMEDA)STrip]$_n$	S	*n*	4	2.77	TMEDA	2.50	[76]
[{Na(12C4)$_2$}$_2$ {Na(THF) (S-2-$NC_5H_4)_2$}{Na (μ-S-2-NC_5H_4)(S-2-NC_5H_4)}]$_2$	S	Mixed	5	2.82	N[a]	2.47	[42]
					THF/12C4	2.47	
[Na$(THF)_2SR_f]_n$	S	*n*	4+2[b]	2.83	THF	2.29	[23]
Na(Et_2O)(THF)Re$(CO)_2(NO)_2$(S^{t}Bu)$_2$OH	S	1	5	2.96	Et_2O/THF	2.30	[78]
Na_2Ru–(1,4,7-(S-2-^{t}Bu-4-C_6H_3)-1,4,7-$N_3C_6H_{15}$)$^{\bullet}CH_2Cl_2{}^{\bullet}$MeOH$^{\bullet}2H_2O$	S	1	6	2.75	N	2.38	[79]
Na$(THF)_2$V(S-2-$NC_5H_4)_4$	S	1	6	2.96	THF	2.31	[80,81]
					N[a]	2.40	
[Na$(THF)_3]_2$U(S^{t}Bu)$_6$	S	1	6	2.96	THF	2.50	[82]
[Na$(THF)_3]_2$U(SPh)$_6$	S	1	6	3.05	THF	2.35	[82]
[Na(THF)Ru$(CO)_2(PPh_3)(SEt)_3]_2$	S	2	5	2.88	THF	2.37	[83,84]
Na$(THF)_3$Fe$(CO)_3(SePh)_3$	Se	1	6	3.18	THF	2.28	[85]
[Na$(py)_2$Sm$(py)_2(SePh)_4]_2$	Se	2	4	2.85	py	2.48	[86]
Na$(TMEDA)_2$TeMes	Te	1	5	3.49	TMEDA	2.54	[87]
[NaEu$(THF)_3(TePh)_3]_n$	Te	*n*	4	3.16	–	–	[88]

[a] Intramolecular coordination.
[b] Additional interactions with two fluorine atoms of *ortho*-CF_3 group observed.

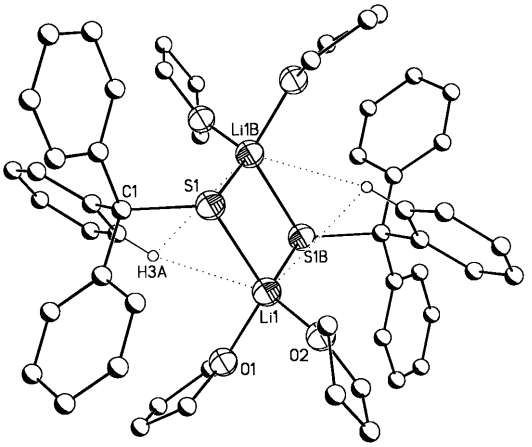

Fig. 2. Graphical representation of $[Li(THF)_2SCPh_3]_2$. Hydrogen atoms, except those showing interactions with the metal center have been omitted for clarity.

stabilization modes was employed, the 12-membered ring species $[LiS\text{-}2,6\text{-}((R)CH(Me)NMe_2)_2C_6H_3]_6$ was obtained. A metal coordination number of four is observed for all hexamers, similar to that found in the majority of lithium chalcogenolates (see Table 3). Accordingly, the two different hexameric structural modes may be understood in terms of preferred metal coordination number.

Monomeric compounds are available, if sterically demanding ligands are used in conjunction with excess donor, as demonstrated by $Li(THF)_3EMes^*$ (E = S, Se, Te) [19,20,47,70]. These compounds feature four-coordinate metal centers, with one metal–ligand interaction. The reduction of ligand bulk resulted in the formation of higher aggregates as demonstrated by the dimers $[Li(THF)_2SCPh_3]_2$ (Fig. 2) [41], and $[Li(THF)_2SCH(SiMe_3)_2]_2$ [18]. The influence of ligand size is also demonstrated

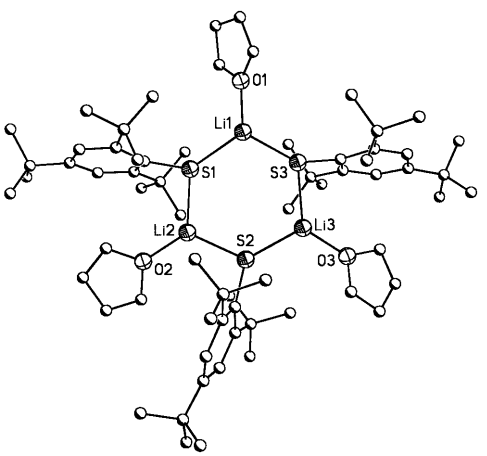

Fig. 3. Graphical representation of $[Li(THF)SMes^*]_3$. Hydrogen atoms have been omitted for clarity.

Table 3
Geometrical details of potassium thiolates, selenolates, and tellurolates

Compound	E	Aggr.	CN	K–E (Å)	D	K–D (Å)	Ref.
K(DB18C6)$SCPh_3 \cdot$ tol	S	1	7+ar	3.13	DB18C6	2.74	[49]
					Arene	3.52–3.96	
K(18C6)$SCPh_3 \cdot 0.5C_6H_6$	S	1	7	3.14	18C6	2.87	[49]
K(DB18C6)SMes*	S	1	7	3.17	DB18C6	2.80	[75]
K(18C6)$SCPh_3 \cdot$ 0.5THF	S	1	7.5	3.16	18C6	2.84	[49]
					THF	3.25	
K(DB18C6)$SCPh_3 \cdot$ 0.5HMPA	S	1	7.5	3.22	DB18C6	2.78	[49]
					HMPA	2.77	
[K(18C6)$(THF)_2$] [SMes*]	S	1	8	–	18C6	2.78	[75]
					THF	2.74	
[K(DB18C6)(THF)STrip]	S	1	8	3.20	DB18C6	2.76	[76]
					THF	2.80	
[K(18C6)(S-2-NC_5H_4)]	S	1	8	3.26	N[a]	2.85	[42]
					18C6	2.91	
[KS-2,6-$Trip_2C_6H_3]_2 \cdot$ tol	S	2	2+ar	3.06	Arene	3.28–3.56	[24]
[$(KSCPh_3)_6(tol)_2$]	S	6	3+ar	3.11	Arene	3.17–3.73	[49]
					tol	3.21–3.84	
			3+ar	3.21	Arene	3.28–3.97	
			4+ar	3.24	Arene	3.12–3.45	
[{KSTrip}$_2${K(THF)STrip}$_2${$K(THF)_2$STrip}$_2$]	S	6	4	3.13	THF	2.60	[76,89]
			5	3.28	THF	2.69	
[$(KSCPh_3)_6(HMPA)_2$]	S	6	4+ar	3.15	HMPA	2.54	[49]
					Arene	3.31–3.53	
			3+ar	3.18	Arene	3.13–3.63	
			4+ar	3.21	Arene	3.10–3.55	
[{KSTrip}$_2${K(THF)STrip}$_2${K(TMEDA)STrip}$_2$]	S	6	4	3.19	THF	2.66	[76,89]
			5	3.26	TMEDA	2.97	
[K(THF)STrip]$_n$	S	*n*	4	3.14	THF	2.68	[76]
[K(THF)S–R_t]$_n$	S	*n*	4	3.17	THF	2.68	[23]
[K(PMDTA)STrip]$_\infty$	S	*n*	5	3.18	PMDTA	2.88	[76]
[{K(μ-S-2-μ-NC_5H_4)}$_2${15C5}]$_n$	S	*n*	9	3.35	N[a]	2.91	[42]
					15C5	3.01	
[$K(CH_3CN)_2Ni(S'Bu)_3]_2$	S	2	5	3.20	CH_3CN	2.83	[90]
[K(18C6)$(THF)_2$]SeMes*	Se	1	8	–	18C6	2.79	[75]
					THF	2.75	
$KSeC_6H_3$-2,6-$Trip_2$	Se	2	2+ar	3.17	Arene	3.26–3.71	[91]
$K_2[Ni(SeCH_2CH_2Se)_2]$•2EtOH	Se	*n*	7	3.47	EtOH	2.79	[92]
K(18C6)TeTrip	Te	1	7	3.50	18C6	2.85	[87]
[$K(THF)_{1.33}$TeTrip]$_n$	Te	n	5	3.50	THF	2.68	[70]

[a] Intramolecular coordination.

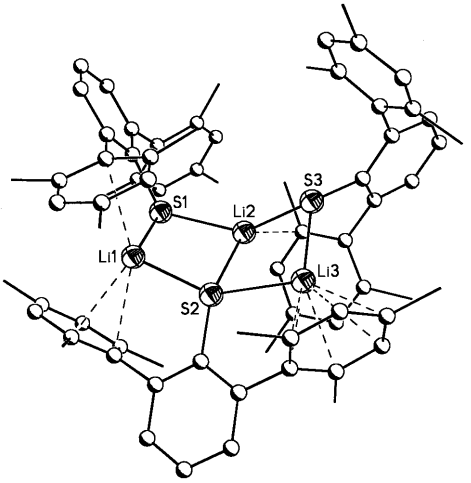

Fig. 4. Graphical representation of [LiS-2,6-$Mes_2C_6H_3$]$_3$. Hydrogen atoms have been omitted for clarity.

with a family of terphenyl derivatives, where the *ortho*-substitution of the ligand determines its steric bulk. Utilization of the sterically very demanding *ortho* substituent 2,4,6-$^i Pr_3C_6H_3$ induced formation of the dimeric [LiS-2,6-$Trip_2C_6H_3$]$_2$ [24]. Replacement of 2,4,6-$^i Pr_3C_6H_3$ by mesityl (2,4,6-$Me_3C_6H_2$) resulted in a higher degree of aggregation, under formation of the trimeric [LiS-2,6-$Mes_2C_6H_2$]$_3$ (Fig. 4) [24]. If mesityl was replaced by phenyl, the tetramer [LiS-2,4,6-$Ph_3C_6H_2$]$_4$ (Fig. 5) [24] was obtained. The oligomeric formulation of the above-mentioned complexes is only observed, if the derivatives are crystallized from toluene. Exposure to Lewis donors results in the break-up of the oligomers and formation of lower aggregates, shown by exposing [LiS-2,4,6-$Ph_3C_6H_2$]$_4$ to excess THF, and isolation of the monomeric Li(THF)$_3$STriph (Fig. 1) as the sole product [46].

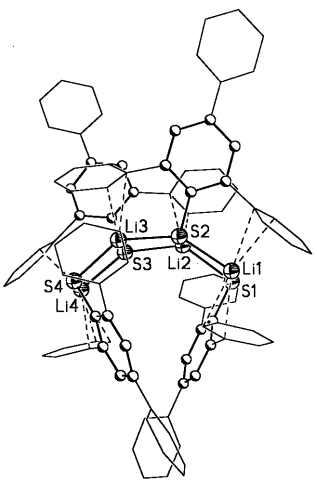

Fig. 5. Graphical representation of [LiSTriph]$_4$. Hydrogen atoms have been omitted for clarity.

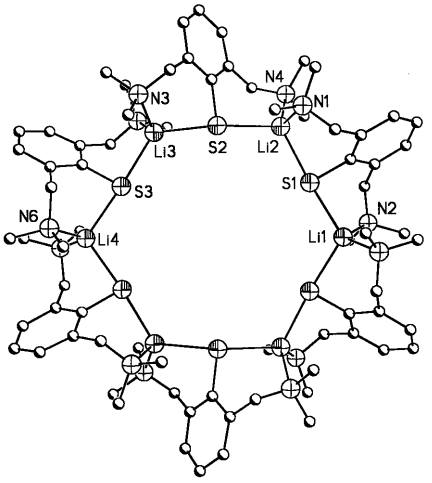

Fig. 6. Graphical representation of $[LiS\text{-}2,6\text{-}(CH_2NMe_2)_2C_6H_3]_6$. Hydrogen atoms have been omitted for clarity.

In addition to ligand size effects, the nature and amount of donor present in the reaction mixture has a significant effect on the structural pattern. Exposing the monomeric $Li(THF)_3EMes^*$ (E = S, Se) to vacuum, even at elevated temperatures, does not result in loss of donor solvent. The trimers $[Li(THF)EMes^*]_3$ (E = S (Fig. 3), Se) are only available if a stoichiometric amount of THF was used in the synthetic scheme, demonstrating the strength of the metal–donor interactions [41,69]. The trimers display almost planar six-membered ring systems comprised of alternating lithium and sulfur/selenium atoms. Each lithium atom is surrounded in a distorted trigonal planar fashion by one THF oxygen and two sulfur/selenium

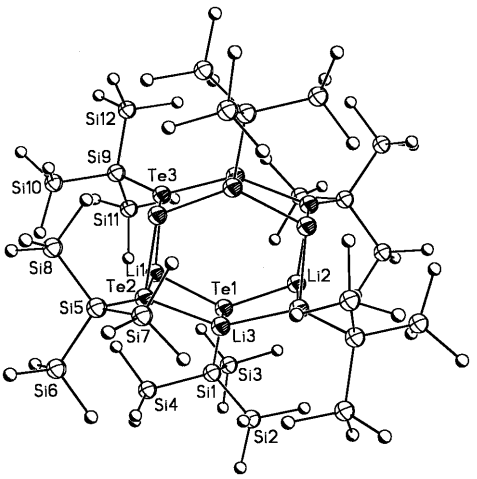

Fig. 7. Graphical representation of $[LiTeSi(SiMe_3)_3]_6$. Hydrogen atoms have been omitted for clarity.

atoms, resulting in three-coordinate lithium centers, and significantly reduced metal–ligand bond lengths, as compared to the four-coordinate monomers. A clear correlation of coordination number and bond length is prevalent throughout the group of lithium chalcogenolates, as also demonstrated by the three-coordinate dimeric tellurolate $[Li(THF)TeSi(SiMe_3)_3]_2$ and the four-coordinate dimer $[Li(THF)_2TeSi(SiMe_3)_3]_2$ [22,72].

Not only the steric bulk of the ligand influences aggregation, but changes in the hapticity of the donor critically affect the structural outcome, as demonstrated by the monomeric Li(PMDTA)STrip, available if the tridentate donor PMDTA is used. If, in contrast, the bidentate TMEDA is utilized, the dimeric $[Li(TMEDA)STrip]_2$ is obtained [41].

The influence of donor hapticity and ligand bulk on structural pattern is further demonstrated in a family of lithium thiolates, where use of a multidentate crown ether in combination with differently sized ligands affects the formation of either separated or contact ion pairs. The formation of separated or contact alkali metal chalcogenolates may be understood as a competition between ligation and solvation processes. Separated alkali metal cations are observed if the interaction between the metal and the Lewis donor is energetically favored over the metal–ligand contact. So far, structural data are available for the separated thiolate, $[Li(12C4)_2][SMes^*]$ [41], shown in Fig. 8, in addition to the tellurolate $[Li(12C4)_2][TeSi(SiMe_3)_3]$ [22]. Interestingly, separation of the cation and anion in both complexes was induced by coordinating the lithium cation to two 12C4 donors, resulting in a sandwich-type arrangement. 12C4 has been previously used to stabilize lithium derivatives involving separated cations [74].

Not only the nature of the donor has an effect on the formation of separated ions, but also the ligand, and even more significantly the combination of both, as expressively shown with the use of two differently sized thiolates SMes* and $SCPh_3$ in conjunction with 12C4. The sterically demanding SMes* affects ion separation, while the smaller $SCPh_3$ resulted in a monomeric species, $Li(12C4)SCPh_3$, isolated independently of the amount of 12C4 present in the reaction mixture [41]. This result clearly shows that the combination of 12C4 with the sterically demanding Mes* ligand affects a metal–ligand bond weakening due to steric repulsion, thus solvation effects are favored.

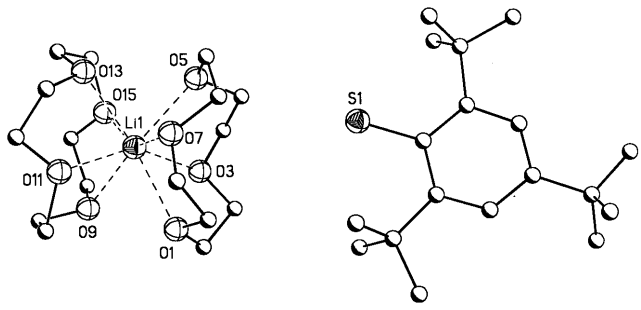

Fig. 8. Graphical representation of $[Li(12C4)_2][SMes^*]$. Hydrogen atoms have been omitted for clarity.

2.3. Sodium, potassium, rubidium and cesium compounds

The number of structurally characterized sodium and potassium chalcogenolates has increased dramatically during the last few years. The first structural characterization of alkali metal thiolates ASMe (A = Li, Na and K), was performed in 1972, using powder diffraction techniques [17]. Single crystal structure data of sodium and potassium chalcogenolates were first reported in 1991, namely the single stranded polymer $[Na(THF)_2SR_f]_n$ and the double stranded, ladder-type polymer $[K(THF)SR_f]_n$ [23]. Over the last few years, several reports delineating factors influencing the structural chemistry of the heavier alkali metal chalcogenolates have appeared in the literature.

A closer look at the chemistry described in these reports indicates that many principles observed for lithium chalcogenolates may be applied towards the heavier alkali metal congeners. However, several factors, specifically the reduced charge density in the heavier metals results in some unique chemistry not observed expressively with the lighter congeners. Several recent publications illuminate the role of the metal, ligand and donors on the structural chemistry observed in the target compounds.

Donor influence on structural pattern was explored with a special emphasis on donor hapticity. In this context, a family of crown ether alkali metal pyridine thiolates was prepared, under the premise that size matching the crown ether with the alkali metal would initiate the formation of simple monomeric structures, whereas odd sized crown ethers would induce more complex structural pattern [42]. This hypothesis was experimentally verified with the isolation of Na(15C5)(S-2-NC_5H_4) and K(18C6)(S-2-NC_5H_4). If size mismatched crown ethers were employed, more complex structural pattern were observed. Examples include the asymmetrically coordinated monomer Na(18C6)(S-2-NC_5H_4), and the unique separated ion quadruple containing sodium centered anions, and cations ligated in a sandwich-fashion by two 12C4 donors, $[\{Na(12C4)_2\}_2\{Na(S\text{-}2\text{-}NC_5H_4)_2(THF)\}\{Na(\mu S\text{-}2\text{-}NC_5H_4)(S\text{-}2\text{-}NC_5H_4)\}]_2$. This unusual 'ate' complex crystallizes with two coordinately different anions in each asymmetric unit, shown in Fig. 9.

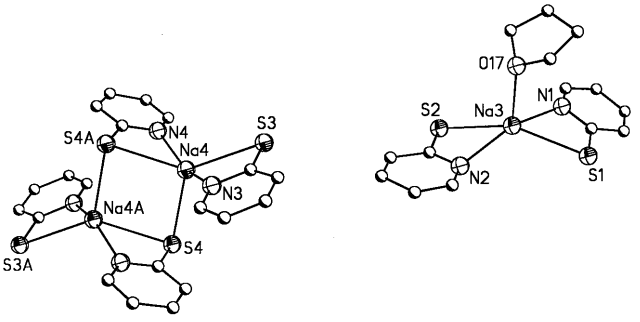

Fig. 9. Graphical representation of $[\{Na(12C4)_2\}_2Na(S\text{-}2\text{-}NC_5H_4)_2$ (THF)$\}\{Na(\mu\text{-}S\text{-}2\text{-}NC_5H_4)(S\text{-}2\text{-}NC_5H_4)\}]_2$. Hydrogen atoms have been omitted for clarity, only the anions are shown.

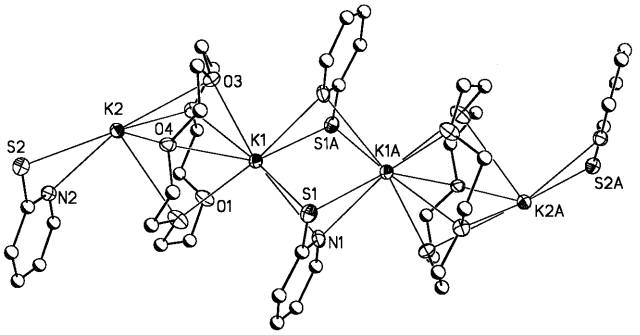

Fig. 10. Graphical representation of $[\{K_2(15C5)(\mu\text{-S-2-}NC_5H_4)_2\}]_n$. Hydrogen atoms have been omitted for clarity. A fragment of the polymer is shown.

The combination of the same ligand system, potassium and 15C5 resulted in the polymeric $[K_2(15C5)(\mu\text{-S-2-}NC_5H_4)_2]_n$, where the crown ether serves as bridging template between KS-2-NC_5H_4 units (Fig. 10). This study shed light on the non-trivial effect of the donor on the structural chemistry: Utilization of a crown ether with a cavity too large to effectively sequester the alkali metal cation led to an asymmetric coordination, while too small a crown cavity induced the formation of either polymeric or ionic species.

Donor influence was further investigated in a family of sodium and potassium Trip thiolate derivatives [76]. This study employed a variety of donors, including THF, bidentate TMEDA, tridentate PMDTA, and multidentate crown ethers. Using PMDTA in connection with sodium resulted in the dimeric [Na(PMDTA)STrip]$_2$, whereas diethyl ether afforded the discrete hexameric box-shaped $[(NaSTrip)_2(Na(Et_2O)STrip)_4]$, shown in Fig. 11.

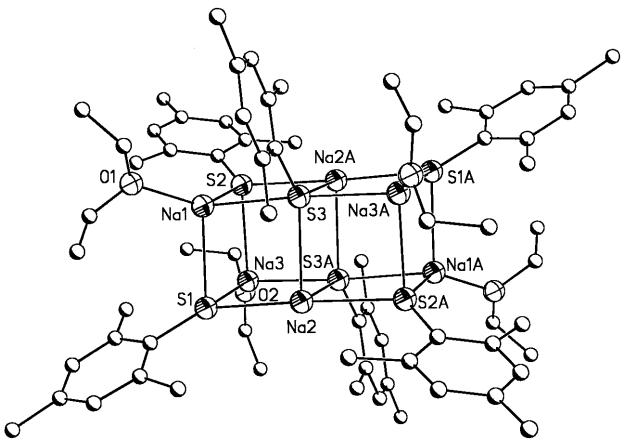

Fig. 11. Graphical representation of $[(NaSTrip)_2(Na(Et_2O)_{2/3}STrip)_4]_6$. Hydrogen atoms have been omitted for clarity.

The hexamer may be described as a discrete double ladder array, or face-fused cuboidal structure with a coordination number of four at all metal centers. The sodium atoms in the central Na_2S_2 ring are connected to four sulfur atoms, those in the outer rings display three sulfur and one diethyl ether coordination. In the presence of TMEDA, the polymeric $[Na(TMEDA)STrip]_n$ is isolated, displaying one dimensional zigzag chains with four-coordinate sodium and three-coordinate sulfur atoms. The overall structural features may be compared with the one-dimensional zigzag polymer $[Na(THF)_2SR_f]_n$ [23]. The trend observed for sodium Trip thiolates is continued in the potassium homologues: the monomer K(DB18C6)-(THF)STrip is clearly the result of crown ether ligation. Utilization of PMDTA yielded the one-dimensional zigzag polymer $[K(PMDTA)STrip]_n$, displaying a chain of alternating five-coordinate potassium and three-coordinate sulfur centers. Further reduction of donor hapticity leads to increased dimensionality in the aggregation pattern as observed in the hexameric box-shaped $[(KSTrip)_2(K(THF)STrip)_2$-$(K(THF)_2STrip)_2]$, (Fig. 12) and $[(KSTrip)_2(K(THF)STrip)_2(K(TMEDA)STrip)_2]$, displaying four- and five-coordinate metal centers [76,89].

Interestingly, the crystallographic data on the hexamer $[(KSTrip)_2(K(THF)$-$STrip)_2(K(THF)_2STrip)_2]$ can be obtained only shortly after the compound was synthesized. Over the course of a few days, the quality of the very thin needles deteriorates, and only X-ray quality crystals of the ladder-type polymer $[K(THF)STrip]_n$ (Fig. 13) remain.

NMR analysis of the reaction product, shortly after the synthesis was performed, showed only one set of signals for each the ligand and the donor, indicating that the asymmetric hexameric structure, observed in the solid state (Fig. 12) is not retained in solution, and the symmetrical ladder-polymer (Fig. 13) is prevalent. If the hexameric array stayed intact, two sets of signals for the Trip groups and THF

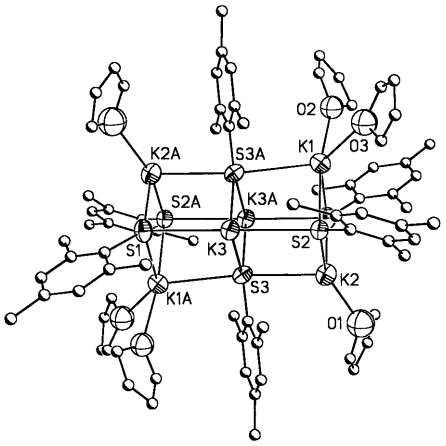

Fig. 12. Graphical representation of $[(KSTrip)_2(K(THF)STrip)_2(K(THF)_2STrip)_2]$. Hydrogen atoms have been omitted for clarity.

donors would be present. The ladder-type polymer $[K(THF)STrip]_n$ shares many structural similarities with the potassium thiolate $[K(THF)R_f]_n$ [23], and the tellurolate $[K(THF)_{1.33}TeTrip]_n$ [70]. The comparison of structural features observed in the aforementioned compounds clearly illuminates the role of metal size, and donor hapticity. The comparison of the one-dimensional zigzag polymers $[Li(py)SCH_2Ph]_n$ [44], $[Na(TMEDA)STrip]_n$ [76], $[Na(THF)_2R_f]_n$ [23], and $[K(PMDTA)STrip]_n$ [76] with the two dimensional ladder polymers $[Li(py)SCH_2Ph]_n$ [44], $[K(THF)STrip]_n$ [76], and $[K(THF)R_f]_n$ [23] nicely demonstrates that either the increase of the metal radius, or alternatively, decrease of ligand bulk results in a higher degree of aggregation.

The influence of secondary metal–ligand interactions on the coordination chemistry of sodium and potassium thiolates was examined in detail by investigating the structural chemistry of a family of sodium and potassium trityl or triphenylsilyl thiolates [49]. Employment of crown ethers afforded the monomeric $K(18C6)(SCPh_3)(solv.)_{0.5}$ (solv. $= C_6H_6$, THF, HMPA) and $K(DB18C6)(SCPh_3)$-(tol), displaying seven-coordinate potassium centers with additional weak donor coordination. 18C6 and DB18C6 effectively preclude oligomerization. Only a few examples of monomeric sodium or potassium chalcogenolates have been reported, all of which rely on crown ether coordination. This is in striking contrast to the lithium analogues, where monomeric compounds are easily obtained by using sterically demanding ligands and excess donor (vide supra). If sodium and potassium chalcogenolates are prepared in the absence of crown ethers, higher aggregates are observed. Remarkably, the reaction of sodium or potassium hydride with tritylthiol or triphenylsilylthiol in toluene, in the absence of crown ether, led to arene stabilized hexamers $[(NaSSiPh_3)_6(tol)_2]$, $[(KSCPh_3)_6(HMPA)_2]$ and $[(KSCPh_3)_6(tol)_2]$, where HMPA or toluene complete the coordination environment at the metal center. A partial and full view of $[(KSCPh_3)_6(tol)_2]$ is shown in Fig. 14(a) and (b).

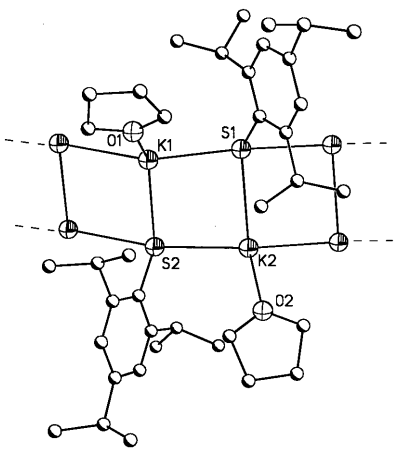

Fig. 13. Graphical representation of $[K(THF)STrip]_n$. Hydrogen atoms have been omitted for clarity, a fragment of the polymer is shown.

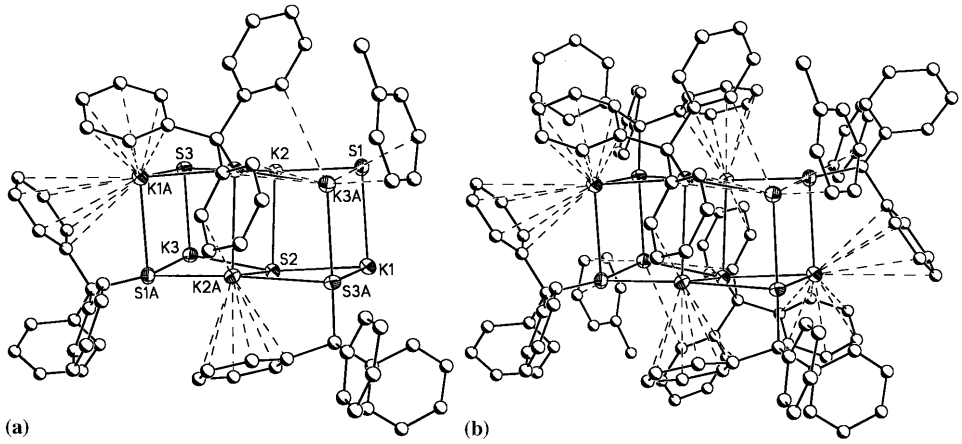

Fig. 14. Partial (a) and full (b) graphical representation of $[(KSCPh_3)_6(tol)_2]$. Hydrogen atoms have been omitted for clarity.

The hexameric aggregates are based on a similar M_6S_6 grid, but significant differences arise in the degree of cation–π interactions about the core structures and the donor ligation at corner positions on each compound. The compact Na_6S_6 framework and greater radial extension of triphenylsilylthiolate prohibits extensive intramolecular cation–π interaction, while simultaneously forming two coordination sites at corner metal positions such that toluene can interact in an η^6 fashion. In contrast, the larger K_6S_6 frame requires extensive intramolecular cation–π interactions. As a result, the two open corner sites cannot accommodate η^6-arene coordination from toluene (rather there is a π-edge orientation); whereas the strongly coordinating HMPA occupies these sites in $[(KSCPh_3)_6(HMPA)_2]$ requiring a reorganization of the trityl periphery. In accord with the known propensity of potassium to sequester toluene to its coordination environment [93], control experiments with competing donors like pyridine, dioxane, or PMDTA in the reaction mixture of KH, $HSCPh_3$ and toluene consistently resulted in the isolation of $[(KSCPh_3)_6(tol)_2]$. This underlines clearly, that toluene is an effective donor for potassium in this series, being displaced only by the strongly ligating HMPA under formation of $[(KSCPh_3)_6(HMPA)_2]$ (Fig. 15).

The capability of alkali metals to form arene interactions is demonstrated expressively in a series of alkali metal terphenyl chalcogenolate derivatives. These ligands combine the capability of arene interactions with extremely large steric demand, making possible the isolation of species with a low degree of aggregation, even if large alkali metal centers are present. Consequently, this work provides the only structural information available on rubidium and cesium chalcogenolates, a summary of which is provided in Table 4.

The combination of ligand steric bulk with concomitant intramolecular arene coordination was utilized to obtain dimeric $[MS\text{-}2,6\text{-}Trip_2C_6H_3]_2$ (M = Na, K, Rb, Cs (Fig. 16)) [24] in addition to the rubidium selenolate $[RbSe\text{-}2,6\text{-}Trip_2C_6H_3]_2$ and the mixed metal $RbAlMe_2S\text{-}2,6\text{-}Trip_2C_6H_3$ [91].

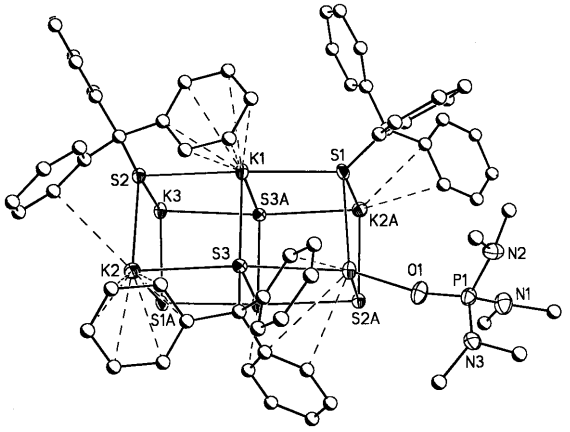

Fig. 15. Partial graphical representation $[(KSCPh_3)_6(HMPA)_2]$. Hydrogen atoms have been omitted for clarity.

Table 4
Geometrical details of rubidium thiolates and selenolates and a cesium thiolate

Compound	E	Aggr.	CN	A–E (Å)	D	A–D (Å)	Ref.
$RbAlMe_2(S\text{-}2,6\text{-}Trip_2C_6H_3)_2$	S	1	2+ar	3.20	Arene	3.29–3.64	[91]
$[RbS\text{-}2,6\text{-}Trip_2C_6H_3]_2 \cdot tol$	S	2	2+ar	3.17	Arene	3.30–3.68	[24]
$[RbSe\text{-}2,6\text{-}Trip_2C_6H_3]_2$	Se	2	2+ar	3.26	Arene	3.31–3.70	[91]
$[CsS\text{-}2,6\text{-}Trip_2C_6H_3]_2$	S	2	2+ar	3.31	Arene	3.53–3.83	[24]

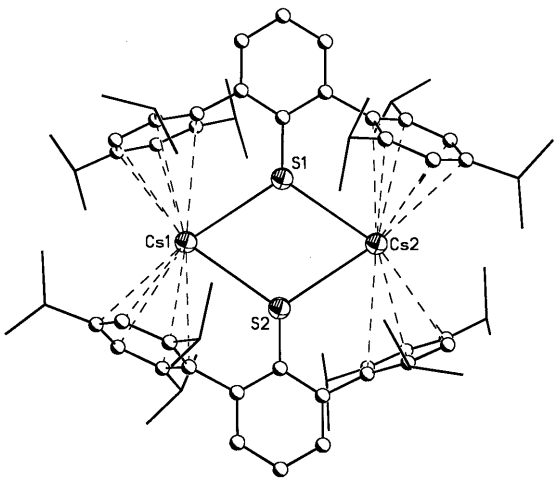

Fig. 16. Graphical representation of $[CsS\text{-}2,6\text{-}Trip_2C_6H_3]_2$. Hydrogen atoms have been omitted for clarity.

The intramolecular arene interaction together with the steric demand of the terphenyl ligand is making the dimeric nature of these compounds possible. The influence of the increasing size of the metal center is demonstrated by an increased degree of arene interaction. The *ortho* substituents on the ligand provide only partial arene coordination for the lighter alkali metal derivatives, but full η^6 arene coordination is observed for the heaviest alkali metal congeners. The increasing degree of π-interaction between the metal and the ligand by descending the group of alkali metals, reflects not only the increased need for steric saturation among the heavier metals, but also the increased trend of the larger metals to interact with the 'soft' π-system.

3. Alkaline earth metal thiolates, selenolates and tellurolates

3.1. Synthetic aspects

During the last few years much work has been devoted towards the development of reliable, reproducible, high-yielding synthetic routes allowing the isolation of pure alkaline earth chalcogenolates. Several different reaction schemes have been developed and tested; summarized in Scheme 3.

Type of reaction:	Equation:	used for:
Transamination	$Ae(NSiMe_3)_2)_2 + 2\ HER \longrightarrow Ae(ER)_2 + 2\ HN(SiMe_3)_2$[a]	Be, Mg, Ca, Sr, Ba
		SR, SeR, TeR
Salt Elimination/Metathesis:	$AeX_2 + 2\ AER \longrightarrow Ae(ER)_2 + 2\ AX$[b]	Be, Mg, Sr
		SR, SeR
Alkane elimination:	$(Bu)_2Ae + 2\ HER \longrightarrow Ae(ER)_2 + 2\ BuH$	Mg
		SR, SeR, TeR
Metallation:	$Ae_{act.} + 2\ HER \longrightarrow Ae(ER)_2 + H_2$[c]	Ca, Sr, Ba
	$Ae_{act.} + REER \longrightarrow Ae(ER)_2$	SR, SeR
Transmetallation	$Ae + Hg(ER)_2 \longrightarrow Ae(ER)_2 + Hg$	Mg
Chalcogen Insertion	$R_2Ae + {}^2/_8\ S_8 \longrightarrow Ae(SR)_2$	Mg, SR

a) E = S, Se, Te, R= alkyl, aryl, silyl, b) X = halide, A = Li, Na, K, c) Activation of metals by solvation in dry, liquid ammonia

Scheme 3. Synthetic routes to alkaline earth metal chalcogenolates.

3.1.1. Transamination

Transamination generally allows the preparation of the target molecules in high yield and purity, employing a variety of solvent and ligand systems. The reaction scheme involves the treatment of alkaline earth amides with chalcogenols. The resulting amine can be removed in vacuum. This reaction route has been used successfully for the synthesis of many target compounds, since it provides a great deal of synthetic flexibility: both donor and non-donor solvents can be used, and different thiols, selenols and tellurols may be employed. The biggest disadvantages are the occasional incomplete amide exchange [94], in addition to the reaction of liberated amine with unreacted acid, as illustrated in Scheme 4. This yield reducing side reaction is most prevalent if small, highly acidic chalcogenols are utilized [95].

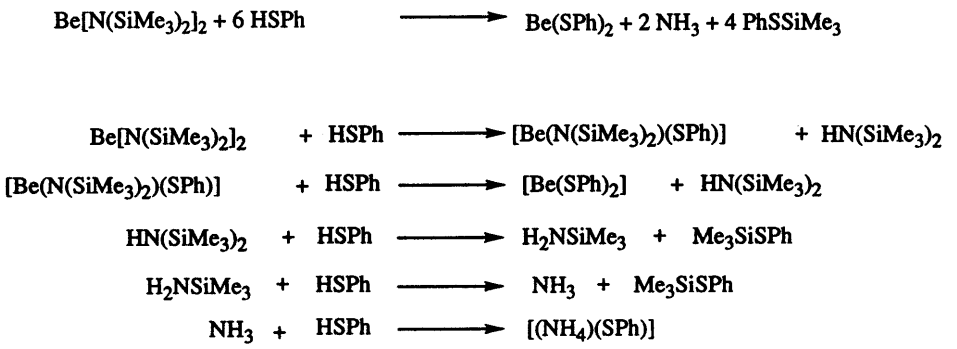

Scheme 4. Yield reducing side reaction observed during transamination.

3.1.2. Salt elimination/metathesis

Alkaline earth chalcogenolates are also accessible by the reaction of alkaline earth halides with alkali chalcogenolates. Only a few target compounds have been prepared using this method since the disadvantages of this methodology far outnumber the availability of alkali metal chalcogenolates and alkaline earth halides. Arnold and Gindelberger describe the reaction between lithium tellurolate and magnesium bromide as problematic [27], an observation shared in our group. Most successful seems to be the reaction of potassium thiolates, selenolates, and tellurolates with the alkaline earth metal iodides. The resulting potassium iodides precipitate in THF.

3.1.3. Alkane elimination

This reaction scheme can be readily used for the preparation of magnesium chalcogenolates bearing a wide variety of ligands and donors. Dibutylmagnesium is commercially available. The reaction of organomagnesium with two equivalents of thiols, selenols or tellurols produces the target molecules in excellent yield and purity. Since alkyl derivatives of the heavier alkaline earth elements are not readily available, this method is currently limited to magnesium and beryllium complexes, though no beryllium chalcogenolate has been synthesized employing this route.

Table 5
Geometrical details of beryllium thiolates

Compound	E	Aggr.	CN	Be–E (Å)	D	Be–D (Å)	Ref.
$Be(Et_2O)(2,6\text{-}Mes_2C_6H_3)(SMes^*)$	S	1	3	1.98	Et_2O	1.62	[100]
$Be(THF)(SMes^*)_2$	S	1	3	1.99	THF	1.59	[28]
$[Be(HMPA)_4][SCPh_3]_2$	S	1	4	–	HMPA	1.59	[101]
$Be(NH_3)(NH_2SiMe_3)(SC_6F_5)_2$	S	1	4	2.11	N	1.74	[101]
$[\{Be(py)(NH_3)(SPh)_2\}_2$ {18C6}]	S	2	4	2.10	NH_3,py	1.731.78	[95]

3.1.4. Metallation

Metallation involves the reaction of alkaline earth metals with (a) chalcogenols or (b) disulfides, diselenides, or ditellurides, in the presence of dry liquid ammonia. The ammonia readily dissolves the heavy alkaline earth metals, proving a highly active surface area. Metallation is especially attractive for the synthesis of selenolates and tellurolates, since the reduction of the diselenide or ditelluride to the highly air-sensitive selenol or tellurol, a low-yielding reaction, can be avoided. It is of notice that the lighter alkaline earth metals require extended reflux times in liquid ammonia to provide good yields [96].

3.1.5. Transmetallation

Transmetallation involves the reaction of mercury chalcogenolates with alkaline earth metals. This procedure has not been applied widely, probably due to the necessary synthesis of the mercury precursor and its toxicity. In addition, activated alkaline earth metal is required to enable a smooth, high-yielding reaction [27].

3.1.6. Chalcogen insertion

The insertion of a chalcogen atom into the metal–carbon bond is based on the long known reaction of elemental sulfur with Grignard reagents. However, only recently the first well characterized magnesium thiolate was described using this route [97]. The lack of stable, easily accessible organocalcium, strontium, and barium derivatives prevents the use of this method for the heavy alkaline earth metal analogs.

3.2. Beryllium compounds

Beryllium chemistry has received little attention, most likely due to the high toxicity of beryllium and its compounds [98,99]. Not surprisingly, this lack of attention is reflected in the small number of structurally characterized beryllium species, especially those displaying bonds with elements located in row three and below in the periodic table. To the best of our knowledge, no structural data on beryllium selenolates or tellurolates are available.

In the sole crystallographic report of a homoleptic beryllium thiolate, the sterically demanding SMes* ligand afforded the three-coordinate monomer

$Be(THF)(SMes^*)_2$ [28] (Table 5). A three-coordinate monomeric formulation was also identified in the mixed alkylberyllium thiolate $Be(Et_2O)(2,6\text{-}Mes_2C_6H_3)(SMes^*)$ [100] again featuring steric stabilization of the metal center. A four-coordinate beryllium environment is observed in $Be(NH_3)(NH_2SiMe_3)(SC_6F_5)_2$ and $[\{Be(py)(NH_3)(SPh)_2\}_2\{18C6\}]$ (Fig. 17) [95], as well as in the dithiocarbamate $[Be(S_2CN(^iPr)_2)_2]$ [102].

Clearly then, the coordination environment of beryllium is dictated by ligand bulk, and three-coordinate species are only obtainable if sterically demanding ligands are utilized. The four-coordinate motif is more common, and expressed with a variety of ligand and donor combinations. $[\{Be(py)(NH_3)(SPh)_2\}_2\{18C6\}]$ (Fig. 17) [95] features two beryllium thiolate moieties associated with one central 18C6 molecule through hydrogen-bonded ammonia species. Completing the four-coordinate environment are two phenylthiolate ligands and one pyridine donor. $Be(NH_3)(NH_2SiMe_3)(SC_6F_5)_2$ features two beryllium thiolate interactions in addition to NH_3 and H_2NSiMe_3 ligation [101]. The beryllium- sulfur contacts in the four-coordinate compounds are somewhat longer than in the three-coordinate $Be(THF)(SMes^*)_2$ [28] and $Be(Et_2O)(2,6\text{-}Mes_2C_6H_3)(SMes^*)$ [100], which can be attributed to the lower coordination number at beryllium, thus confirming the previously observed correlation of increased coordination numbers and bond lengths.

3.3. Magnesium compounds

Magnesium chalcogenolates have been discussed in review articles most recently in 1997 [5,6], with a literature coverage until 1996. As evidenced by Table 6, many compounds have been added to the list of magnesium chalcogenolates since 1996, warranting an update and comparison of old and newly obtained data.

About 10 years ago, the first magnesium thiolate was reported by van Koten et al. [25]. Since then, about two-dozen analogs involving a variety of ligands and

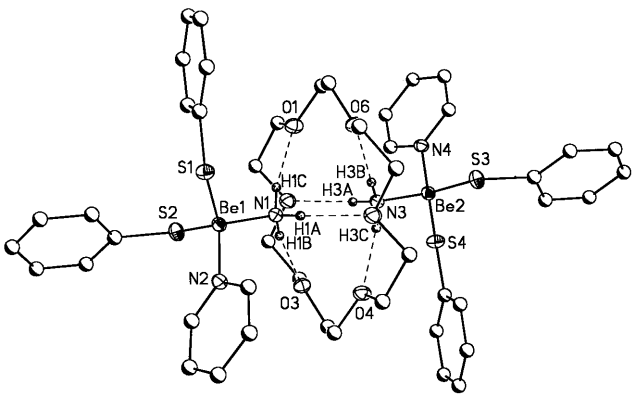

Fig. 17. Graphical representation of $[\{Be(py)(NH_3)(SPh)_2\}_2)\{18C6\}]$. Hydrogen atoms, except those on NH_3 have been omitted for clarity.

Table 6
Geometrical details of magnesium thiolates, selenolates, and tellurolates

Compound	E	Aggr.	CN	Mg–E (Å)	D	Mg–D (Å)	Ref.
$Mg(S\text{-}2,6\text{-}Trip_2C_6H_3)_2$	S	1	2+ar	2.33	Arene	2.69–2.79	[91]
$[Mg(Tp^{p\text{-}Tol})SH]$	S	1	4	2.35	$N(Tp^{p\text{-}Tol})$	2.10	[103]
$Mg(Et_2O)_2(SMes^*)_2$	S	1	4	2.39	Et_2O	2.07	[104]
$Mg(HMPA)_2(SSiPh_3)_2$	S	1	4	2.43	HMPA	1.94	[101]
$Mg(THF)_2(N(SiMe_3)_2)(SMes^*)$	S	1	4	2.43	THF	2.05	[94]
$[(C_7H_9NH)]_2[Mg(SC_6F_5)_4]$	S	1	4	2.45	–	–	[105]
$Mg(py)_3(SC_6F_5)$	S	1	5	2.49	py	2.17	[105]
$Mg(py)_2(S\text{-}2\text{-}NC_5H_4)_2$	S	1	6	2.62	N[a]	2.17	[105]
					py	2.20	
$Mg(py)_4(SPh)_2$	S	1	6	2.63	py	2.29	[105]
$Mg(py)_4(SC_6F_5)_2$	S	1	6	2.65	py	2.28	[106]
$Mg(15C5)(SCPh_3)_2$	S	1	7	2.66	15C5	2.18	[107]
$[Mg(15C5)(THF)_2]\ [SMes^*]_2$	S	1	7		15C5	2.17	[107]
					THF	2.09	
$[Mg(STriph)_2]_2$	S	2	3+ar	$2.35^t 2.46^{br}$	Arene	2.56, 2.80	[104]
$[(CuMes)_4(\mu\text{-}SC_6H_4(CH(Me)NMe_2)\text{-}2)_2(Mg(SC_6H_4(CH(Me)NMe_2)\text{-}2))_2]$	S	2	4	2.38^t	N[a]	2.18	[25]
				2.43^{br}			
$[Mg(THF)(SMes^*)_2]_2$	S	2	4	2.37^t	THF	2.03	[94]
				2.50^{br}			
$[Mg(THF)(N(SiMe_3)_2)(STrip)]_2$	S	2	4	2.51^{br}	THF	2.05	[94]
$[Mg(THF)(N(SiMe_3)_2)(SPh)]_2$	S	2	4	2.53^{br}	THF	2.03	[94]
$[Mg(SC_6H_4\text{-}2\text{-}CH_2NMe_2)_2]_2$	S	2	5	2.45^t	N[a]	2.25	[97]
				2.55^{br}			
$[Mg_3(py)_6(\eta^2\text{-}SPh)_6]$	S	3	6	2.61^{br}	py	2.22	[105]
$[Mg(Tp^{p\text{-}Tol})SeH]$	Se	1	4	2.46	$N(Tp^{p\text{-}Tol})$	2.10	[103]
$[Mg(Tp^{p\text{-}Tol})SePh]$	Se	1	4	2.50	$N(Tp^{p\text{-}Tol})$	2.11	[108]
$Mg(THF)_2(SeMes^*)_2$	Se	1	4	2.54	THF	2.02	[104]
$Mg(TRMPSI)(SeSi(SiMe_3)_3)_2$	Se	1	5	2.49	TRMPSI	2.66	[29]
$Mg(THF)_2(TeSi(SiMe_3)_3)_2$	Te	1	4	2.72	THF	2.04	[27,29]

[a] Intramolecular coordination.
[br] Bridging.
[t] Terminal.

donors have been synthesized and structurally characterized, providing critical information about association and aggregation trends within this group of compounds. The chemistry of magnesium selenolates and tellurolates has received a lesser degree of attention, and only about half-a-dozen well characterized compounds have appeared in the literature.

The magnesium-chalcogen bond has a strong ionic component, as indicated by the excellent agreement of experimentally obtained magnesium-chalcogen bond lengths with the sum of ionic radii for Mg^{2+} and E^{2-} (E = S, Se, Te) [109]. This view is further supported by ab initio calculations by Pappas [38], who describes the Mg–S interactions as predominately ionic. Pappas also calculated the Mg–S bond distance in a hypothetical, two-coordinate $Mg(SH)_2$ to be 2.324 Å, a value which agrees well with crystallographic data for magnesium thiolates with comparable coordination numbers.

The high ionic component of the metal–ligand bond often results in low solubility, and a tendency towards polymerization in the target compounds, especially if small ligands are utilized. Accordingly, sterically demanding ligands and/or strong donors are prevalent in magnesium chalcogenolate chemistry.

As shown in Table 6, bonding interactions between the magnesium center and the chalcogenolate ligands are observed in all compounds, except $[Mg(15C5)(THF)_2][SMes^*]_2$ (Fig. 18), where an isolated cation and separated anions are observed [107]. Arnold et al. mention a related species [29], the tellurolate $[Mg(12C4)_2][TeSi(SiMe_3)_3]_2$, but no crystallographic evidence is supporting this suggestion. Ligand size in conjunction with donor hapticity has been made responsible for the formation of separated lithium chalcogenolates (vide supra), and analogous factors contribute towards the formation of the magnesium congeners.

The formation of the separated ions is typically associated with a dramatic change in physical properties, such as solubility or volatility, greatly affecting their use as precursor materials. Accordingly, a systematic study investigating factors

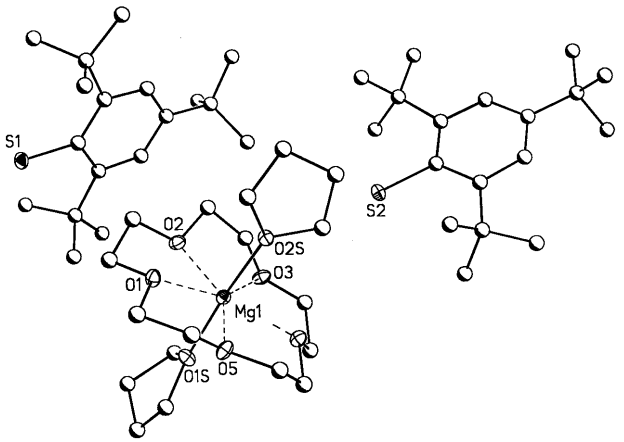

Fig. 18. Graphical representation of $[Mg(15C5)(THF)_2][SMes^*]_2$. Hydrogen atoms have been omitted for clarity.

responsible for the formation of separated ions is crucial, specifically due to the potential of the target molecules as precursor materials. Ligand bulk in conjunction with multidentate donors are the major deciding factor in the formation of separated ions, as demonstrated by comparing the seven-coordinate $Mg(15C5)(SCPh_3)_2$ (Fig. 19) [107] with the separated $[Mg(15C5)(THF)_2][SMes^*]_2$ (Fig. 18). Synthetic procedures for both compounds were identical, with the exception of differently sized ligands. Apparently, the crown ether coordination about magnesium prohibits the close approach of the sterically demanding SMes* ligand, thus weakening a potential metal–ligand bond. Since the formation of contact and separated ions may be understood as a competition between solvation and ligation processes, solvation by the smaller THF donors is preferred, and the separated species $[Mg(15C5)(THF)_2][SMes^*]_2$ is observed.

Magnesium chalcogenolates may exhibit a variety of coordination numbers, ranging from two (plus arene) to seven. The coordination environment about the metal seems to be mainly affected by the steric demand of the ligand. A single compound with coordination number two (plus arene) has been reported. The sterically very cumbersome terphenyl ligand 2,6-$Mes_2C_6H_2$ made possible the monomeric formulation observed in $Mg(S\text{-}2,6\text{-}Mes_2C_6H_3)_2$, displaying bend S–Mg–S geometry, short magnesium–sulfur bonds, and significant metal–arene interaction [91]. A combination of steric bulk and arene interactions were also responsible for the dimeric $[Mg(STriph)_2]_2$ (Fig. 20), whose magnesium centers are connected to three thiolate ligands, in addition to arene interactions to the *ortho* phenyl substituents of the ligand [104].

The importance of ligand steric bulk on coordination chemistry becomes further evident when borne in mind that $Mg(S\text{-}2,6\text{-}Mes_2C_6H_3)_2$ and $[Mg(STriph)_2]_2$ are the only magnesium chalcogenolates displaying these low coordination numbers. The majority of magnesium target compounds display higher coordination numbers (Table 6). Selected examples of four-coordinate magnesium chalcogenolates include the monomers $Mg(Et_2O)_2(SMes^*)_2$ (Fig. 21) [104], and $Mg(HMPA)_2(SSiPh_3)_2$ [101], the dimer $[Mg(THF)(SMes^*)_2]_2$ (Fig. 22) [94], the selenolate $Mg(THF)_2(SeMes^*)_2$ [104], and the tellurolate $Mg(THF)_2(TeSi(SiMe_3)_3)_2$ [27]. The common theme

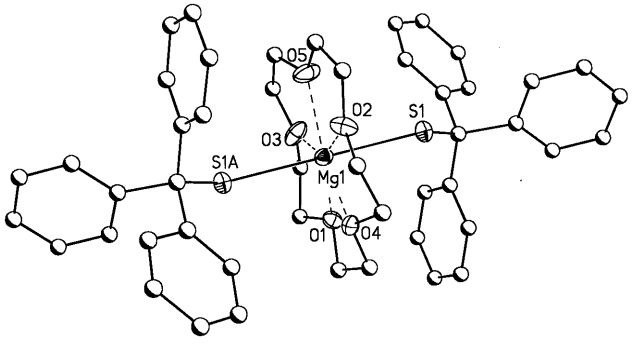

Fig. 19. Graphical representation of $Mg(15C5)(SCPh_3)_2$. Hydrogen atoms have been omitted for clarity.

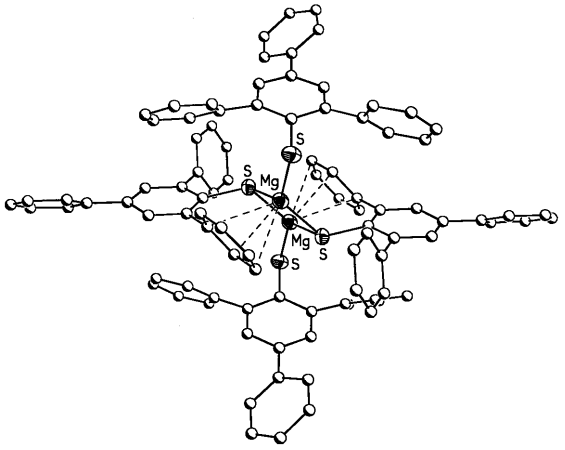

Fig. 20. Graphical representation of $[Mg(STriph)_2]_2$. Hydrogen atoms have been omitted for clarity.

among these compounds is the presence of sterically demanding ligands in conjunction with donor molecules. The tendency for strong donor coordination can be illustrated by comparing the presumably three-coordinate dimer $[Mg(SMes^*)_2]_2$ (according to NMR results) [104] with the four-coordinate dimer $[Mg(THF)(SMes^*)_2]_2$ [94] and the monomeric four-coordinate $Mg(Et_2O)_2(SMes^*)_2$ [104], which are available by using either, a stoichiometric, or excess amount of donor. This may be compared with related lithium thiolates, where the addition of THF to the tetrameric $[LiSTriph]_4$ [24] resulted in the break-up of the oligomer and quantitative formation of the monomeric $Li(THF)_3STriph$ [46]. Analogously, the trimer $[Li(THF)EMes^*]_3$ (E = S, Se) is isolated if a stoichiometric amount of donor is applied [41,69], in the presence of excess donor, the monomeric $Li(THF)_3EMes^*$ is the sole product [19,20,47].

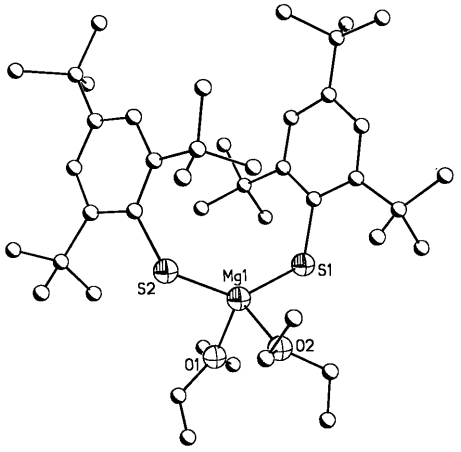

Fig. 21. Graphical representation of $Mg(SMes^*)_2(OEt_2)_2$. Hydrogen atoms have been omitted for clarity.

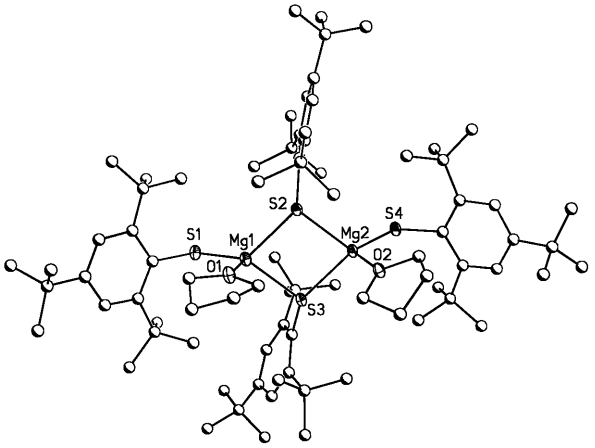

Fig. 22. Graphical representation of $[Mg(THF)(SMes^*)_2]_2$. Hydrogen atoms have been removed for clarity.

Donor and ligand influence are specifically addressed in a study focussing on magnesium thiolates bearing small ligands, such as SPh and SC_6F_5 [105]. Polymerization is prevented, and solubility assured by utilizing the strong donors pyridine and 2,6-lutidine. The formation of the monomeric, five-coordinate $Mg(py)_3(SC_6F_5)_2$ is clearly a consequence of ligand steric bulk, since an analogous reaction with HSC_6H_5 and vast excess of pyridine resulted in the formation of the octahedral $Mg(py)_4(SPh)_2$. Interestingly, two of the pyridine donors exhibit significantly shorter magnesium nitrogen distances than the remaining two. Consequently, a reaction was carried out with the intention to synthesize a species with only three pyridine donors attached to the metal center. However, when a reduced amount of pyridine was utilized, the trimeric $Mg_3(py)_6(\mu^2\text{-SPh})_6$, (Fig. 23) and not the

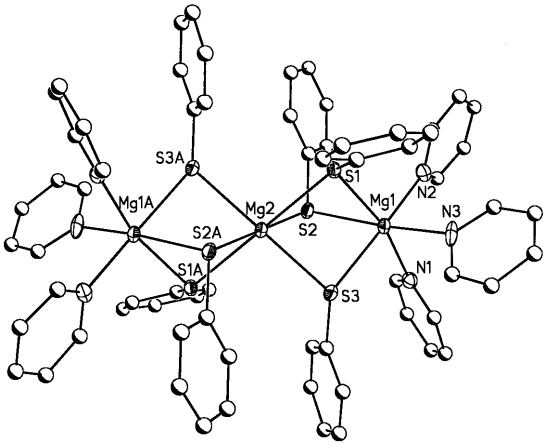

Fig. 23. Graphical representation of $Mg_3(py)_6(\mu^2\text{-SPh})_6$. Hydrogen atoms have been omitted for clarity.

monomeric five-coordinate $Mg(py)_3(SPh)_2$, was reproducibly isolated in good yield and purity.

Apparently, the steric bulk of SPh is not sufficient to stabilize a five-coordinate metal center. In addition, fluorinated ligands have been shown previously to stabilize low coordination numbers, probably due to electronic repulsion between neighboring ligands. All magnesium centers in $Mg_3(py)_6(\mu^2\text{-}SPh)_6$ exhibit octahedrally coordinate metal centers: the central magnesium unit is bound to six bridging sulfur thiolate atoms, while the two outer magnesium atoms are connected to three bridging sulfur atoms in addition to three terminal pyridine molecules, resulting in a ligand–donor stoichiometry of 1:1. The trimer represents a rare example of a main group derivative in which octahedrons are connected via shared faces. To further evaluate the coordination environment of magnesium thiolates, a larger nitrogen donor 2,6-Me_2-pyridine (2,6-lutidine) was used in conjunction with HSC_6F_5. Surprisingly, the magnesiate thiolate $[C_7H_9NH]_2[Mg(SC_6F_5)_4]$ was isolated as the sole product. The compound can be synthesized in a rational fashion by treating $(C_4H_9)_2Mg$ with four equivalents of thiol in the presence of 2,6-lutidine. The anions display a distorted tetrahedrally coordinate metal center, where magnesium is ligated by four thiolate groups with magnesium–sulfur distances slightly elongated in comparison with neutral four-coordinate magnesium thiolates. It is believed that the bond elongation is due to the anionic nature of the complex. Anionic complexes of the alkaline earth metals are rare, and are generally favored if ligands with low Lewis basicity are connected to the metal center. The Lewis acidic metal center will interact with an increased number of ligands to compensate for its electron deficiency [110].

This study clearly shows the non-trivial coordination chemistry in magnesium chalcogenolates. Simple changes in regards to ligand or donor steric requirement do not necessarily result in simple, expected changes in the composition or conformation of the final product. Similar trends were observed in the related alkali derivatives, again, underscoring the similarities of both groups of compounds.

3.4. Calcium compounds

Even so that $Ca(THF)_4(TeSi(SiMe_3)_3)_2$ (Fig. 24) was published independently by two groups several years ago [26,27,29], the number of structurally characterized calcium chalcogenolates remains small, and is currently limited to four thiolates, three selenolates, and the above mentioned tellurolate (Table 7). In addition to this small group of structurally characterized compounds, few other chalcogenolates have been mentioned, but no information is available regarding their solid-state structures [111]. This lack of data is in sharp contrast to the potential use of calcium chalcogenolates in a variety of technically important applications.

The calcium–sulfur bond may be described as mainly ionic, as supported by ab initio calculations [38], and the excellent agreement between the sum of Ca^{2+} and E^{2-} (E = S, Se, Te) radii and experimentally observed Ca–E bond lengths [109]. As a lower limit for calcium thiolato bonding, the linear, two-coordinate gas phase species $[Ca(SH)_2]$ has a calculated Ca–S interaction of 2.650 Å [38]. This is a

Table 7
Geometrical details of calcium thiolates, selenolates, and tellurolates

Compound	E	Aggr.	CN	Ca–E (Å)	D	Ca–D (Å)	Ref.
$Ca(py)_4(SC_6F_5)_2$	S	1	6	2.85	py	2.52	[96]
Ca(18C6) $(SMes^*)_2$	S	1	8	2.82	18C6	2.59	[96]
$[Ca(18C6)(NH_3)_3][SMes^*]_2$	S	1	9	–	18C6	2.67	[96]
					NH_3	2.51	
$Ca(THF)_4(SMes^*)_2$	S	1	6	2.82	THF	2.44	[112]
$[Ca(PMDTA)(OH)(SMes^*)]_2$	S	2	6	2.84	PMDTA	2.64	[101]
					OH^{br}	2.25	
$[Ca(HMPA)_4(C(=S)NOPh)]$ $[(NC(=S)OPh)_4Co_2Cl]$	S	1	6	2.94	N^a	2.55	[113]
					HMPA	2.29	
$Ca(THF)_4(SeMes^*)_2$	Se	1	6	2.93	THF	2.43	[112]
[Ca(18C6)(THF)(SeMes*)] [SeMes*]	Se	1	8	3.00	THF	2.40	[112]
					18C6	2.57	
$[Ca(18C6)(HMPA)_2][SeMes^*]_2$	Se	1	8	–	18-C-6	2.67	[112]
					HMPA	2.25	
$Ca(TeSi(SiMe_3)_3)_2(THF)_4$	Te	1	6	3.20	THF	2.39	[26,27,29]

[a] Intramolecular coordination.
[br] Bridging.

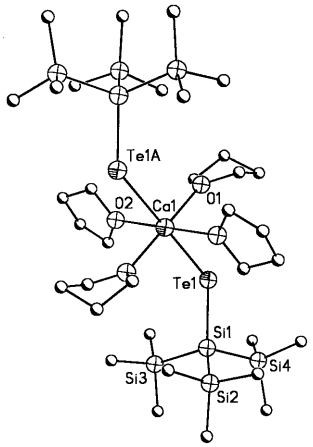

Fig. 24. Graphical representation of $Ca(THF)_4(TeSi(SiMe_3)_3)_2$. Hydrogen atoms have been omitted for clarity.

considerably shorter value than seen in the solid-state structure of any experimentally observed thiolate, however, it should be kept in mind that the calculated bond length reflects a two-coordinate metal center.

The commonly observed coordination number in calcium chalcogenolates is at least six, but may be as high as nine. Typically, compounds with a coordination number of six are observed if simple donors are employed, as verified in the thiolates $Ca(py)_4(SC_6F_5)_2$ [96], $Ca(THF)_4(SMes^*)_2$ [112], and [Ca(P-MDTA)(OH)$(SMes^*)]_2$ [101], the selenolate $Ca(THF)_4(SeMes^*)_2$ [112], and the tellurolate $Ca(THF)_4(TeSi(SiMe_3)_3)_2$ [26,27]. These compounds display slightly distorted octahedral metal centers.

If multidentate donors like crown ethers are employed, compounds with coordination numbers above six for calcium are obtained, as observed in the eight-coordinate $Ca(18C6)(SMes^*)_2$ [96]. In addition, the crown ether may induce the formation of separated ions, similar to the above mentioned magnesium or alkali metal analogs. Three different types of ion association modes are possible (Scheme 1), with two cation–anion contacts, separated cations and anions, or an intermediate situation with one cation–anion linkage and one separated anion. Remarkably, all three association modes are verified among calcium chalcogenolates and can be rationalized on the basis of steric and bond strength considerations.

Using 18C6 in conjunction with the sterically demanding SMes* yielded the eight-coordinate $Ca(18C6)(SMes^*)_2$, displaying two remarkably different calcium–sulfur contacts (2.775(3) and 2.851(2) Å), and two different calcium–sulfur–carbon angles (154.0(3) and 119.1(2)°). Interestingly, the wider Ca–S–C angle coincides with the shorter Ca-S bond, while the narrower Ca–S–C angle is associated with the longer Ca-S distance. The correlation between the Ca–S bond length and the angle at sulfur indicates some degree of steric repulsion between the *ortho* ^{t}butyl groups on the ligand with the crown ether, thus preventing

a close approach of the ligand, and the formation of a short, strong Ca–S bond. Therefore, it is not surprising, that the introduction of stronger donors than THF induce the formation of separated species, as observed in $[Ca(18C6)(NH_3)_3][SMes^*]_2$ [96] and $[Ca(18C6)(HMPA)_2][SeMes^*]_2$ [112]. The formation of the intermediate [Ca(18C6)(THF)(SeMes*)][SeMes*] [112] might be explained on the basis of reduced Ca–Se bond strength as compared to the sulfur analogs. As a consequence, solvation processes, as compared to ligation, will be energetically more favorable. These three compounds represent two types of ion association: $[Ca(18C6)(NH_3)_3][SMes^*]_2$ and $[Ca(18C6)(HMPA)_2][SeMes^*]_2$ display separated ions, while in [Ca(18C6)(THF)(SeMes*)][SeMes*] one cation–anion bond and one separated anion is observed. Interestingly, $Ca(18C6)(SMes^*)_2$ and $[Ca(18C6)(NH_3)_3][SMes^*]_2$ were prepared in an identical manner, with the exception that the separated species was isolated after an extraction with THF at room temperature, while $Ca(18C6)(SMes^*)_2$ was obtained after hot solvent work-up (see Fig. 25(a) and (b)). The NH_3 donors in the separated species can be removed by a short exposure to vacuum, or by extraction with hot solvent, as evidenced by IR and NMR spectroscopic studies. If NH_3 is added at room temperature or below, the separated species is formed quantitatively. The facile formation of separated ion

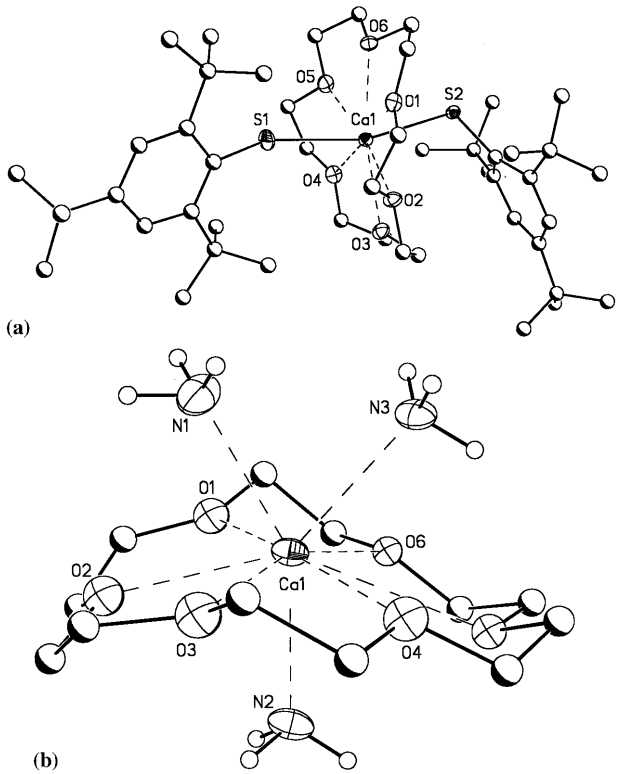

Fig. 25. Graphical representation of $Ca(18C6)(SMes^*)_2$ (a) and $[Ca(18C6)(NH_3)_3][SMes^*]_2$ (b). Hydrogen atoms, except those on NH_3 have been omitted for clarity. In (b) only the cation is shown.

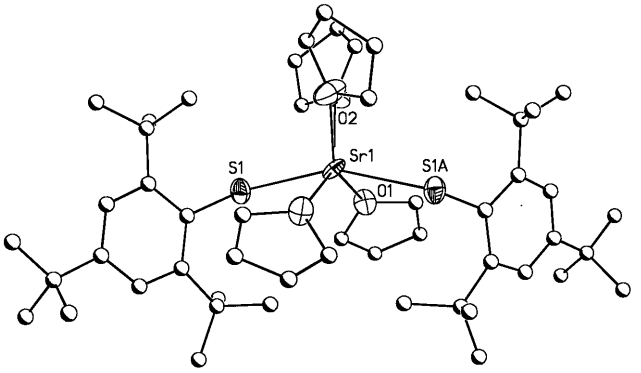

Fig. 26. Graphical representation of $Sr(THF)_4(SMes^*)_2$. Hydrogen atoms have been omitted for clarity.

triples underscores the high ionic character and weak nature of the Ca-S bond. This argument is in agreement with calculations by Pappas [38] and experimental work by Mingos et al. [114].

A comparison of structural data between calcium and the lighter alkaline earth congeners, indicates a trend towards higher coordination numbers in the heavier alkaline earth derivatives, which can clearly be attributed to the increased metal radius. The direct comparison of coordination geometry between beryllium, magnesium, and calcium compounds bearing identical ligands and donors, shows a relatively smooth trend, with an increase in coordination number from three to six as observed in the three-coordinate $Be(THF)(SMes^*)_2$ [28], the four-coordinate $Mg(Et_2O)_2(SMes^*)_2$ [104] and the octahedral $Ca(THF)_4(SMes^*)_2$ [112].

3.5. Strontium and barium compounds

Few examples of strontium and barium thiolates, selenolates and tellurolates have appeared in the literature despite their importance in various technical applications [34,35,37,111]. The group of strontium derivatives is limited to $Sr(THF)_4(SMes^*)_2$ (Fig. 26) [115], $[Sr(18C6)(HMPA)_2][SMes^*]_2$ [116], $[Sr(NH_3)(py)(SCEt_3)_2]_n$ (Fig. 27) [111], $Sr(THF)_4(SeMes^*)_2$ [115], and $Sr(TMEDA)(SeSi(SiMe_3)_3)_2$ [29]. Examples of corresponding barium analogs include $Ba(THF)_4(SMes^*)_2$ [112], [Ba(18C6)(HMPA)SMes*][SMes*] (Fig. 28) [116], $[Ba(H_2O)_4(H_2$2,4,6-$S_3C_3N_3)_2]_n$ [117], $Ba(THF)_4(SeMes^*)_2$, $[Ba(18C6)(HMPA)_2][[SeMes^*]_2$, (Fig. 29), $Ba(18C6)(SeTrip)_2$ (Fig. 30), $[Ba(py)_3(THF)(SeTrip)_2]_2$, (Fig. 31) [112], and $Ba(py)_5(TeSi)SiMe_3)_3)_2$ (Fig. 32) [29]. Selected geometrical details are provided in Tables 8 and 9.

The overall structural pattern observed in strontium and barium chalcogenolate chemistry is very comparable to that of calcium. The increased ionic radius of the heavier metals may induce an extended coordination sphere. This assumption is verified by the observation that strontium and barium derivatives have a minimum coordination number of six, which in some cases is extended to eight or nine (see

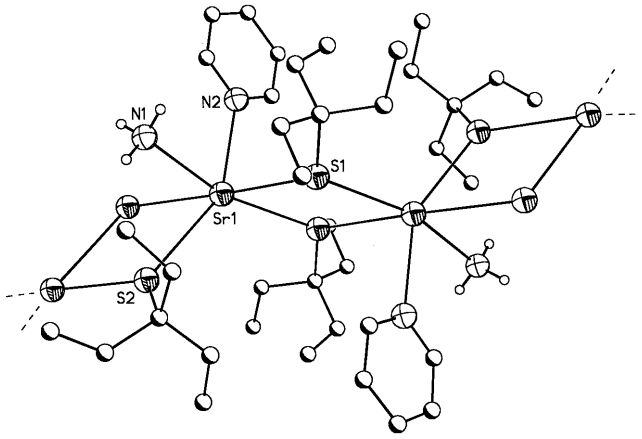

Fig. 27. Graphical representation of $[Sr(NH_3)(py)(SCEt_3)_2]_n$, showing part of the polymeric chain. Hydrogen atoms, except those on NH_3 have been omitted for clarity.

Tables 8 and 9). A common pattern among strontium and barium chalcogenolates is the presence of sterically demanding ligands to maintain solubility and prevent the formation of insoluble, polymeric compounds.

All strontium and barium compounds, synthesized without crown ether, display metal–ligand bonds, as observed in $Sr(THF)_4(EMes^*)_2$ (E = S (Fig. 26), Se) [115], $[Sr(NH_3)(py)(\mu\text{-}SCEt_3)_2]_n$, (Fig. 27) [111], $Sr(TMEDA)_2(SeSi(SiMe_3)_3)_2$ [29], $Ba(THF)_4(EMes^*)_2$ (E = S, Se), the dimeric $[Ba(THF)(py)_3(SeTrip)_2]_2$ (Fig. 31) [112] and $Ba(py)_5(TeSi(SiMe_3)_3)_2$ (Fig. 32) [29]. Among these compounds, the commonly observed coordination environment is distorted octahedral, with the exception of the seven-coordinate selenolate $[Ba(THF)(py)_3(SeTrip)_2]_2$ and the tellurolate

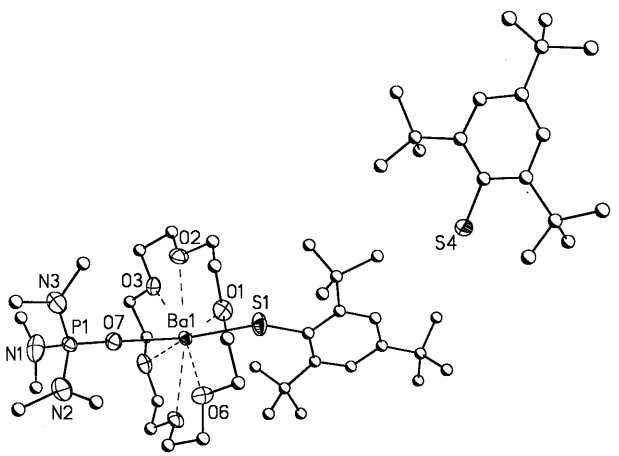

Fig. 28. Graphical representation of [Ba(18C6)(HMPA)(SMes*)] [SMes*]. Hydrogen atoms have been omitted for clarity.

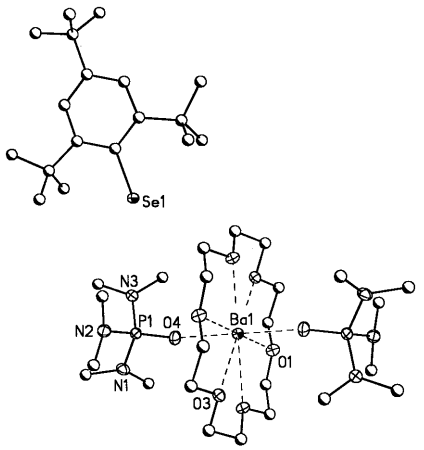

Fig. 29. Graphical representation of $[Ba(18C6)(HMPA)_2][SeMes^*]_2$. Hydrogen atoms have been omitted for clarity. Only one anion is shown.

$Ba(py)_5(TeSi(SiMe_3)_3)_2$, which display distorted pentagonal bipyramidal coordination environments. The increased coordination number in the barium selenolate dimer and the tellurolate can be attributed to the relative steric demand of the ligand. The selenolate dimer contains the smaller -2,4,6-$^iPr_3C_6H_2$ rather than the larger -2,4,6-$^tBu_3C_6H_2$ ligand, moreover, the relatively long barium–selenium distance results in further reduced steric presence of the ligand, enabling the approach of additional donor molecules. A further indication for the relatively small size of the SeTrip ligand is the isolation of $Ba(18C6)(SeTrip)_2$ (Fig. 30). Apparently, the smaller SeTrip ligand is not involved in significant steric repulsion between the crown ether and the ligand, enabling the formation of a compound with two barium–selenium bonds. The long barium–tellurium distance (3.38 Å) in

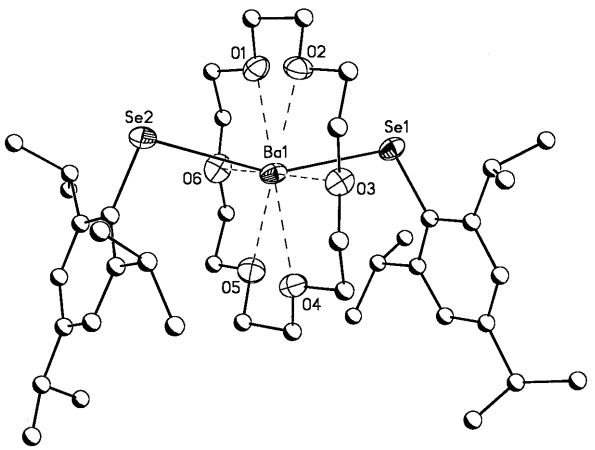

Fig. 30. Graphical representation of $Ba(18C6)(SeTrip)_2$. Hydrogen atoms have been omitted for clarity.

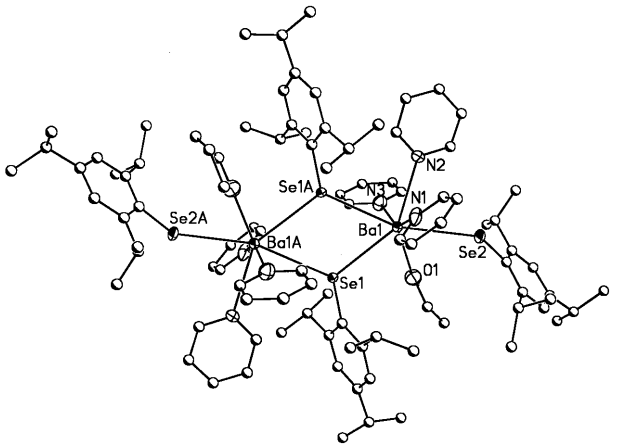

Fig. 31. Graphical representation of $[Ba(py)_3(THF)(SeTrip)_2]_2$. Hydrogen atoms have been omitted for clarity.

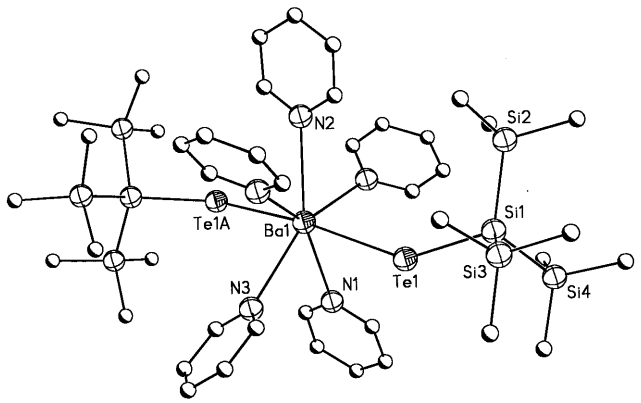

Fig. 32. Graphical representation of $Ba(py)_5(TeSi(SiMe_3)_3)_2$. Hydrogen atoms have been omitted for clarity.

Table 8
Geometrical details of strontium thiolates and selenolates

Compound	E	Aggr.	CN	Sr–E (Å)	D	Sr–D (Å)	Ref.
$Sr(THF)_4(SMes^*)_2$	S	1	6	2.95	THF	2.57	[115]
$[Sr(18C6)(HMPA)_2][SMes^*]_2$	S	1	8	–	18C6	2.72	[116]
					HMPA	2.42	
$[Sr(NH_3)(py)(SCEt_3)_2]_n$	S	*n*	6	3.00	NH_3	2.73	[111]
					py	2.75	
$Sr(THF)_4(SeMes^*)_2$	Se	1	6	3.07	THF	2.56	[115]
$Sr(TMEDA)_2(SeSi(SiMe_3)_3)_2$	Se	1	6	2.94	TMEDA	2.70	[29]

Table 9
Geometrical details of barium thiolates, selenolates, and tellurolates

Compound	E	Aggr.	CN	Ba–E (Å)	D	Ba–D (Å)	Ref.
$Ba(THF)_4(SMes^*)_2$	S	1	6	3.13	THF	2.73	[112]
$Ba(HMPA)_3(C(=S)NOPh)$	S	1	7	3.31	HMPA	2.60	[118]
$Ba(HMPA)_3[C(S)NNNNaph]_2$	S	1	7	3.31	HMPA	2.59	[119]
[Ba(18C6)(HMPA)(SMes*)] [SMes*]	S	1	8	3.02	18C6		[116]
					HMPA	2.59	
$Ba(H_2O)_4(H_2$2,4,6-$S_3C_3N_3)_2$	S	*n*	9	3.4–3.62	N[a]	2.99–3.05	[117]
$Ba(THF)_4(SeMes^*)_2$	Se	1	6	3.28	THF	2.73	[112]
$[Ba(18C6)(HMPA)_2]$ $[SeMes^*]_2$	Se	1	8	–	18C6	2.79	[112]
					HMPA	2.59	
$Ba(18C6)(SeTrip)_2$	Se	1	8	3.23	18C6	2.78	[112]
$[Ba(py)_3(THF)(SeTrip)_2]_2$	Se	2	7	3.30, 3.42[br]	py	2.87	[112]
				3.28[t]	THF	2.82	
$Ba(py)_5(TeSi(SiMe_3)_3)_2$	Te	1	7	3.38	py	2.89	[29]

[a] Intramolecular coordination.
[br] Bridging.
[t] Terminal.

$Ba(py)_5(TeSi(SiMe_3)_3)_2$ can also be made responsible for the decreased steric presence of the tellurolate ligand, enabling the approach of a fifth pyridine donor.

The presence of a crown ether results in compounds with higher coordination numbers, while enabling the isolation of separated species. As observed previously, the formation of separated ions depends on several factors: ligand size, the presence of auxiliary donors, metal–ligand and metal–donor bond strength, and the size of the metal center.

A clear demonstration of the large size of the strontium and barium centers is the required presence of crown ethers in combination with strong, sterically demanding donors, such as HMPA to affect the formation of separated cations and anions. This is in contrast to analogous beryllium, magnesium, or calcium derivatives, where separated ions are obtained in the presence of a strong donor, as observed in $[Be(HMPA)_4][SCPh_3]_2$, or a crown ether in the presence of THF and/or NH_3, as observed in $[Mg(15C5)(THF)_2][SMes^*]_2$, $[Ca(18C6)(THF)(SeMes^*)][SeMes^*]$ and $[Ca(18C6)(NH_3)_3][SMes^*]_2$. The larger cations, strontium and barium, require the combined presence of crown ether and sterically demanding donors to obtain the necessary steric saturation of the metal center. This is demonstrated with the isolation of the separated $[Sr(18C6)(HMPA)_2][SMes^*]_2$, and $[Ba(18C6)(HMPA)_2]$-$[[SeMes^*]_2$ and the intermediate [Ba(18C6)(HMPA)SMes*][SMes*]. Reduction of the ligand size, and/or omission of HMPA results in compounds with metal–ligand contacts as observed in $Ba(18C6)(SeTrip)_2$ (Fig. 30).

The above list of strontium and barium chalcogenolates represents three different ion association modes: with two metal–ligand contacts, without a metal–ligand bond, and compounds with one metal–ligand bond, representing an intermediate state between contact and separated species (Scheme 1). This arrangement is the least known association mode for alkaline earth derivatives. Only two compounds, the above mentioned calcium selenolate [Ca(18C6)(THF)(SeMes*)][SeMes*], and the barium thiolate [Ba(18C6)(HMPA)SMes*][SMes*] represent this rare state. Interestingly, both compounds are observed even if a very large excess of donor (THF or HMPA) is present in the reaction mixture.

4. Conclusion

Over the last decade a steadily increasing amount of information regarding the chemistry of alkali and alkaline earth metal chalcogenolates has been obtained, illuminating the role of critical structure determining factors as the metal, the ligand, and the donor on the structure and consequently, function of the target compounds. Metal influence is mainly limited to its size and charge density, while the ligand determines the structural outcome by its steric demand, the ligand atom bound to the metal center, and consequently, the metal–ligand bond strength as well as the ligands' capability for secondary interactions with the metal center. The donor determines structural chemistry by its base strength, size, and, if applicable, hapticity.

The analysis of structural trends observed for the alkali and alkaline earth derivatives indicates that multiple factors contribute and compete to varying degrees towards the structural chemistry of the target species. Accordingly, more than one variable has to be considered if a structural outcome needs to be predicted. Due to the non-trivial interplay of various parameters it is not always straightforward to accurately predict structural pattern, as demonstrated with the structural characterization of $[\{Na(12C4)_2\}_2\ \{Na(THF)\ (S\text{-}2\text{-}NC_5H_4)_2\}\{Na\ (\mu\text{-}S\text{-}2\text{-}NC_5H_4)(S\text{-}2\text{-}NC_5H_4)\}]_2$, isolated if a crown ether too small (12C4) for the sodium cation was used in the synthetic scheme (see Fig. 9). Another example of an unexpected structural pattern is the magnesiate thiolate $[C_7H_9NH]_2\ [Mg(SC_6F_5)_4]$, isolated if 2,6-lutidine was employed, rather than the smaller pyridine, which allowed the isolation of the neutral, five-coordinate $Mg(py)_3(SC_6F_5)_3$.

Despite the fact that the structural chemistry cannot always be accurately predicted, the body of work accumulated over the last decade resulted in a much improved understanding of the role of the different structure determining factors. In the majority of cases, an accurate structural prediction is possible, since several unifying structural principles have been recognized. As a general rule, lower aggregates will be observed if metal–donor interaction (solvation) is energetically preferred over additional metal–ligand coordination. If, however, metal–ligand moieties are preferred, the formation of higher aggregates is likely to be observed. Another important structure determining factor is the steric demand of the ligand, and generally, compounds with lower coordination numbers are observed if the

steric demand of the ligand is increased. Sterically demanding ligands also play a major role in preventing polymerization reactions by blocking the coordination of additional ligands needed for the polymer formation. An important structural pattern, the formation of separated ions is also facilitated by the presence of sterically demanding ligands. However, the major deciding factor in the formation of separated species is the presence of a multidentate donor, such as crown ether, providing the critically needed cation steric saturation. Depending on the metal size, additional donors, such as THF, NH_3 or HMPA need to be present to further sterically saturate the separated cations and affect the separation of metal and ligand(s).

Even so, that not all structure determining factors are well understood, and it remains difficult to accurately weigh the effects of all contributing factors, it is generally possible to accurately predict the structural chemistry and estimate physical properties, which have a direct impact on the function of the candidate molecules as precursor materials in various applications.

Acknowledgements

We gratefully acknowledge the enthusiasm and efforts of our coworkers Dr Scott Chadwick, Weijie Teng, Sona Dalal and Kelly Davis, who carried out much of the synthetic work described here. Our collaborators Drs Mathias O. Senge and Bruce Noll helped with the collection of X-ray crystallography data during the times when our instrument was down. We are also thankful for the financial support provided by Syracuse University, the Petroleum Research Fund administered by the American Chemical Society (ACS-PRF 28361-G3), the National Science Foundation (CHE-94-09446 and CHE-97-02246), and the Deutsche Forschungsgemeinschaft (Postdoctoral stipend for U.E.). We gratefully acknowledge funds from NSF (CHE-95-27898), the W.M. Keck Foundation, and Syracuse University which made possible the purchase of the X-ray diffractometer at Syracuse University.

Appendix A. Abbreviations

A	alkali metal
Ae	alkaline earth metal
bipy	bipyridyl
CN	coordination number
Cp	cylopentadienide
Cp*	pentamethylcylopentadienide
D	donor
DB18C6	dibenzo-18-crown-6
DME	dimethoxyethane
en	ethylenediamine
HMPA	hexamethylphosphoramide
Mes	mesityl, 2,4,6-$Me_3C_6H_2$

Mes*	2,4,6-$tBu_3C_6H_2$
Ph	phenyl
PMDTA	*N*,*N*,*N*′,*N*″,*N*″-pentamethyldiethylenetriamine
py	pyridine
R_f	2,4,6-$(CF_3)_3C_6H_2$
THF	tetrahydrofuran
TMEDA	*N*,*N*,*N*′,*N*′-tetramethylethylenediamine
tol	toluene
$Tp^{p\text{-}tol}$	tris(3-*p*-tolylpyrazolyl)hydroborate
Trityl	triphenylmethyl
TRMPSI	tris(dimethylphosphinomethyl)-^{t}butylsilane
Trip	2,4,6-$^i Pr_3C_6H_2$
Triph	2,4,6-$Ph_3C_6H_2$
12C4	12-crown-4
15C5	15-crown-5
18C6	18-crown-6

References

[1] W.N. Setzer, P.v R. Schleyer, Adv. Organomet. Chem. 24 (1985) 353.
[2] J.R. Dilworth, J. Hu, Adv. Inorg. Chem. 40 (1993) 411.
[3] F. Pauer, P.P. Power, in: A.-M. Sapse, P.v.R. Schleyer (Eds.), Lithium Chemistry: A Theoretical and Experimental Overview, Wiley, New York, 1995, p. 295.
[4] J. Arnold, Progr. Inorg. Chem. 43 (1995) 353.
[5] M.D. Janssen, D.M. Grove, G. van Koten, Progr. Inorg. Chem. 46 (1997) 97.
[6] K. Ruhlandt-Senge, Commun. Inorg. Chem. 19 (1997) 351.
[7] Z. Hou, Y. Wakatsuki, Chem. Eur. J. 3 (1997) 1005.
[8] M.G. Stanton, M.R. Gagné, J. Am. Chem. Soc. 119 (1997) 5075.
[9] Z. Hou, A. Fujita, H. Yamazaki, Y. Wakatsuki, J. Am. Chem. Soc. 118 (1996) 2503.
[10] F.M. Mackenzie, R.E. Mulvey, J. Am. Chem. Soc. 118 (1996) 4721.
[11] K.W. Henderson, D.S. Walther, P.G. Williard, J. Am. Chem. Soc. 117 (1995) 8680.
[12] P.A. van der Schaaf, M.P. Hogerheide, D.M. Grove, A.L. Spek, G. van Koten, J. Chem. Soc. Chem. Commun. (1992) 1703.
[13] M. Shibasaki, H. Sasai, T. Arai, Angew. Chem. Int. Ed. Engl. 36 (1997) 1236.
[14] W.J. Evans, R.E. Golden, J.W. Ziller, Inorg. Chem. 32 (1993) 3041.
[15] M.P. Hogerheide, S.N. Ringelberg, M.D. Janssen, J. Boersma, A.L. Spek, G. van Koten, Inorg. Chem. 35 (1996) 1195.
[16] P.A. van der Schaaf, J.T.B.H. Jastrzebski, M.P. Hogerheide, W.J.J. Smeets, A.L. Spek, J. Boersma, G. van Koten, Inorg. Chem. 32 (1993) 4111.
[17] E. Weiss, U. Joergens, Chem. Ber. 105 (1972) 481.
[18] M. Aslam, R.A. Bartlett, E. Block, M.M. Olmstead, P.P. Power, G.E. Sigel, J. Chem. Soc. Chem. Commun. (1985) 1674.
[19] K. Ruhlandt-Senge, P.P. Power, Inorg. Chem. 30 (1991) 3683.
[20] W.W. duMont, S. Kubiniok, L. Lange, S. Pohl, W. Saak, I. Wagner, Chem. Ber. 124 (1991) 1315.
[21] G. Becker, K.W. Klinkhammer, S. Lartiges, P. Böttcher, W. Pohl, Z. Anorg. Allg. Chem. 613 (1992) 7.
[22] P.J. Bonasia, D.E. Gindelberger, B.O. Dabbousi, J. Arnold, J. Am. Chem. Soc. 114 (1992) 5209.
[23] S. Brooker, F.T. Edelmann, T. Kottke, H.W. Roesky, G.M. Sheldrick, D. Stalke, K.H. Whitmire, J. Chem. Soc. Chem. Commun. (1991) 144.

[24] M. Niemeyer, P.P. Power, Inorg. Chem. 35 (1996) 7264.
[25] D.M. Knotter, W.J.J. Smeets, A.L. Spek, G. van Koten, J. Am. Chem. Soc. 112 (1990) 5895.
[26] G. Becker, K.W. Klinkhammer, W. Schwarz, M. Westerhausen, T. Hildenbrand, Z. Naturforsch. Teil B 47 (1992) 1225.
[27] D.E. Gindelberger, J. Arnold, J. Am. Chem. Soc. 114 (1992) 6242.
[28] K. Ruhlandt-Senge, R.A. Bartlett, M.M. Olmstead, P.P. Power, Inorg. Chem. 32 (1993) 1724.
[29] D.E. Gindelberger, J. Arnold, Inorg. Chem. 33 (1994) 6293.
[30] H. Okuyama, K. Nakano, T. Miyajima, K. Akimoto, Jpn. J. Appl. Phys. 30 (1991) L1620.
[31] K. Kondo, H. Okuyama, A. Ishibashi, Appl. Phys. Lett. 64 (1994) 3434.
[32] J. Suda, Y. Kawakami, S. Fujita, Jpn. J. Appl. Phys. 33 (1994) L290.
[33] K. Kondo, M. Ukita, H. Yshida, Y. Kishita, H. Okuyama, S. Ito, T. Ohata, K. Nakano, J. Appl. Phys. 76 (1994) 2621.
[34] C.K. Lowe-Ma, T.A. Vanderah, T.E. Smith, J. Solid State Chem. 117 (1995) 363.
[35] P.N. Kumta, S.H. Risbud, J. Mater. Sci. 29 (1994) 1135.
[36] A.P. Purdy, A.D. Berry, C.F. George, Inorg. Chem. 36 (1997) 3370.
[37] M.M. Yuta, W.B. White, J. Electrochem. Soc. 139 (1992) 2347.
[38] J.A. Pappas, J. Am. Chem. Soc. 100 (1978) 6023.
[39] CCDC, Cambridge Crystallographic Data Centre, CSD System, update April 1999 (1994).
[40] W.A. Wojtczak, P.F. Fleig, M.J. Hampden-Smith, Adv. Organomet. Chem. 40 (1996) 215.
[41] K. Ruhlandt-Senge, U. Englich, M.O. Senge, S. Chadwick, Inorg. Chem. 35 (1996) 5820.
[42] S. Chadwick, K. Ruhlandt-Senge, Chem. Eur. J. 9 (1998) 1768.
[43] E. Weiss, Angew. Chem. Int. Ed. Engl. 32 (1993) 1501.
[44] A.J. Banister, W. Clegg, W.R. Gill, J. Chem. Soc. Chem. Commun. (1987) 850.
[45] M.D. Janssen, E. Rijnberg, C.A. de Wolf, M.P. Hogerheide, D. Kruis, H. Kooijman, A.L. Spek, D.M. Grove, G. van Koten, Inorg. Chem. 35 (1996) 6735.
[46] K. Ruhlandt-Senge, P.P. Power, Bull. Soc. Chim. Fr. 129 (1992) 594.
[47] G.A. Sigel, P.P. Power, Inorg. Chem. 26 (1987) 2819.
[48] W. Clegg, J.E. Davies, M.R.J. Elsegood, E. Lamb, J.J. Longridge, J.M. Rawson, R. Snaith, A.E.H. Wheatley, Inorg. Chem. Commun. 1 (1998) 58.
[49] S. Chadwick, U. Englich, K. Ruhlandt-Senge, Organometallics 16 (1997) 5792.
[50] D.R. Armstrong, A.J. Banister, W. Clegg, W.R. Gill, J. Chem. Soc. Chem. Commun. (1986) 1672.
[51] D.R. Armstrong, R.E. Mulvey, D. Barr, R.W. Porter, P.R. Raithby, T.R.E. Simpson, R. Snaith, D.S. Wright, K. Gregory, P. Mikulcik, J. Chem. Soc. Dalton Trans. (1991) 765.
[52] J.J. Ellison, P.P. Power, Inorg. Chem. 33 (1994) 4231.
[53] N. Froelich, P.B. Hitchcock, J. Hu, M.F. Lappert, J.R. Dilworth, J. Chem. Soc. Dalton Trans. (1996) 1941.
[54] R. Amstutz, T. Laube, W.B. Schweizer, D. Seebach, J.D. Dunitz, Helv. Chim. Acta 67 (1984) 224.
[55] D.R. Armstrong, R.E. Mulvey, D. Barr, R. Snaith, D.S. Wright, W. Clegg, S.M. Hodgson, J. Organomet. Chem. 362 (1989) C1.
[56] H. Kawaguchi, K. Tatsumi, R.E. Cramer, Inorg. Chem. 35 (1996) 4391.
[57] K. Tatsumi, I. Matsubara, Y. Inoue, A. Nakamura, R.E. Cramer, G.J. Tagoshi, J.A. Golen, J.W. Gilje, Inorg. Chem. 29 (1990) 4928.
[58] K. Tatsumi, T. Amemiya, H. Kawaguchi, K. Tani, J. Chem. Soc. Chem. Commun. (1993) 773.
[59] K. Ruhlandt-Senge, Dissertation, Marburg, 1991.
[60] H. Schumann, I. Albrecht, E. Hahn, Angew. Chem. Int. Ed. Engl. 24 (1985) 985.
[61] H. Schumann, I. Albrecht, M. Gallagher, E. Hahn, C. Muchmore, J. Pickardt, J. Organomet. Chem. 349 (1988) 103.
[62] R.H. Heyn, D.W. Stephan, Inorg. Chem. 34 (1995) 2804.
[63] F. Becke, T. Ruffer, R. Boese, D. Blaser, D. Steinborn, J. Organomet. Chem. 545 (1997) 169.
[64] F.M. MacDonnell, K. Ruhlandt-Senge, J.J. Ellison, R.H. Holm, P.P. Power, Inorg. Chem. 34 (1995) 1815.
[65] H. Kawaguchi, K. Tatsumi, A. Nakamura, J. Chem. Soc. Chem. Commun. (1995) 111.
[66] M. Berardini, T.J. Emge, J.G. Brennan, J. Chem. Soc. Chem. Commun. (1993) 1537.
[67] D.V. Khasnis, M. Buretea, T.J. Emge, J.G. Brennan, J. Chem. Soc. Dalton Trans. (1995) 45.

[68] K.E. Flick, P.J. Bonasia, D.E. Gindelberger, J.E.B. Katari, D. Schwartz, Acta Crystallogr. Sect. C 50 (1994) 674.
[69] K. Ruhlandt-Senge, P.P. Power, Inorg. Chem. 32 (1993) 4505.
[70] P.J. Bonasia, J. Arnold, J. Organomet. Chem. 449 (1993) 147.
[71] H. Gornitzka, S. Besser, R. Herbst-Irmer, U. Kilimann, F.T. Edelmann, Angew. Chem. Int. Ed. Engl. 31 (1992) 1260.
[72] P.J. Bonasia, V. Christou, J. Arnold, J. Am. Chem. Soc. 115 (1993) 6777.
[73] G. Becker, K.W. Klinkhammer, W. Massa, Z. Anorg. Allg. Chem. 619 (1993) 628.
[74] P.P. Power, Acc. Chem. Res. 21 (1988) 147.
[75] S. Chadwick, U. Englich, K. Ruhlandt-Senge, C. Watson, A. Bruce, M. Bruce, J. Chem. Soc. Dalton Trans (2000) in press.
[76] U. Englich, S. Chadwick, K. Ruhlandt-Senge, Inorg. Chem. 37 (1998) 283.
[77] D.J. Rose, Y.D. Chang, Q. Chen, P.B. Kettler, J. Zubieta, Inorg. Chem. 34 (1995) 3973.
[78] S.E. Nefedov, A.A. Sidorov, H. Berke, I.L. Eremenko, Izv. Akad. Nauk. SSSR. Ser. Khim. (1998) 1030.
[79] K. Mochizuki, F. Kesting, T. Weyhermüller, K. Wieghardt, C. Butzlaff, J. Chem. Soc. Chem. Commun. (1994) 909.
[80] J.G. Reynolds, S.C. Sendlinger, A.M. Murray, J.C. Huffman, G. Christou, Angew. Chem. Int. Ed. Engl. 31 (1992) 1253.
[81] J.G. Reynolds, S.C. Sendlinger, A.M. Murray, J.C. Huffman, G. Christou, Inorg. Chem. 34 (1995) 5745.
[82] P.C. Leverd, M. Lance, M. Nierlich, J. Vigner, M. Ephritikhine, J. Chem. Soc. Dalton Trans. (1993) 2251.
[83] P.G. Jessop, S.J. Rettig, B.R. James, J. Chem. Soc. Chem. Commun. (1991) 773.
[84] P.G. Jessop, S.J. Rettig, C.L. Lee, B.R. James, Inorg. Chem. 30 (1991) 4617.
[85] W.F. Liaw, C.H. Lai, C.K. Lee, G.H. Lee, S.M. Peng, J. Chem. Soc. Dalton Trans. (1993) 2421.
[86] M. Berardini, T.J. Emge, J.G. Brennan, Inorg. Chem. 34 (1995) 5327.
[87] P.J. Bonasia, J. Arnold, J. Chem. Soc. Chem. Commun. (1990) 1299.
[88] D.V. Khasnis, M. Brewer, J. Lee, T.J. Emge, J.G. Brennan, J. Am. Chem. Soc. 116 (1994) 7129.
[89] K. Ruhlandt-Senge, U. Englich, J. Chem. Soc. Chem. Commun. (1996) 147.
[90] A. Müller, G. Henkel, Z. Naturforsch. Teil B 50 (1995) 1464.
[91] M. Niemeyer, P.P. Power, Inorg. Chim. Acta 263 (1997) 201.
[92] C.A. Marganian, N. Baidya, M.M. Olmstead, P.K. Mascharak, Inorg. Chem. 31 (1992) 2992.
[93] D.A. Dougherty, Science 271 (1996) 163.
[94] W. Teng, U. Englich, K. Ruhlandt-Senge, Inorg. Chem. submitted.
[95] S. Chadwick, U. Englich, K. Ruhlandt-Senge, Angew. Chem. Int. Ed. Engl. 37 (1998) 3007.
[96] S. Chadwick, U. Englich, B. Noll, K. Ruhlandt-Senge, Inorg. Chem. 37 (1998) 4718.
[97] M.D. Janssen, R. van der Rijst, A.L. Spek, D.M. Grove, G. van Koten, Inorg. Chem. 35 (1996) 3436.
[98] D.H. Groth, Environ. Res. 21 (1980) 56.
[99] A.L. Reeves, in: L. Friberg, G.F. Nordberg, V.B. Vouk, B. Velimir (Eds.), Handbook of Toxicological Metals, Elsevier, Amsterdam, 1979, pp. 329–343.
[100] M. Niemeyer, P.P. Power, Inorg. Chem. 36 (1997) 4688.
[101] S. Chadwick, K. Ruhlandt-Senge, unpublished results.
[102] H. Nöth, D. Schlosser, Chem. Ber. 121 (1988) 1711.
[103] P. Ghosh, G. Parkin, Chem. Commun. (1996) 1239.
[104] K. Ruhlandt-Senge, Inorg. Chem. 34 (1995) 3499.
[105] S. Chadwick, U. Englich, M.O. Senge, B.C. Noll, K. Ruhlandt-Senge, Organometallics 17 (1998) 3077.
[106] W. Teng, K. Ruhlandt-Senge, unpublished results.
[107] S. Chadwick, U. Englich, K. Ruhlandt-Senge, Inorg. Chem. 38 (1999) 6289.
[108] P. Ghosh, G. Parkin, Polyhedron 16 (1997) 1255.
[109] R.D. Shannon, Acta Crystallogr. A 32 (1976) 751.
[110] N.S. Poonia, A.V. Bajaj, Chem. Rev. 5 (1979) 389.

[111] A.P. Purdy, A.D. Berry, C.F. George, Inorg. Chem. 36 (1997) 3370.
[112] U. Englich, K. Ruhlandt-Senge, B. Costisella, in preparation, (2000).
[113] M.G. Davidson, M. Gerloch, S.C. Llewellyn, P.R. Raithby, R. Snaith, J. Chem. Soc. Chem. Commun. (1993) 1363.
[114] V.-C. Arunasalam, D.M.P. Mingos, J.C. Plakatouras, I. Baxter, M.B. Hursthouse, K.M.A. Malik, Polyhedron 14 (1995) 1105.
[115] K. Ruhlandt-Senge, K. Davis, S. Dalal, U. Englich, M.O. Senge, Inorg. Chem. 34 (1995) 2587.
[116] S. Chadwick, U. Englich, K. Ruhlandt-Senge, Chem. Commun. (1998) 2149.
[117] K. Henke, D.A. Atwood, Inorg. Chem. 37 (1998) 224.
[118] P. Mikulcik, P.R. Raithby, R. Snaith, D.S. Wright, Angew. Chem. Int. Ed. Engl. 30 (1991) 428.
[119] F.A. Banbury, M.G. Davidson, A. Martin, P.R. Raithby, R. Snaith, K.L. Verhorevoort, D.S. Wright, J. Chem. Soc. Chem. Commun. (1992) 1152.